AD-A078 008 SYRACUSE UNIV NY F/G 9/3
MEASUREMENT OF ELECTRICAL CONDUCTIVITY IN CARBON/EPOXY COMPOSIT--ETC(U)
OCT 79 W F WALKER , R E HEINTZ F30602-76-C-0121
UNCLASSIFIED RADC-TR-79-255 NL

| OF |
AD
A078008

END
DATE
FILMED
1-80
DDC

LEVEL II

RADC-TR-79-255
Phase Report
October 1979

MEASUREMENT OF ELECTRICAL CONDUCTIVITY IN CARBON/EPOXY COMPOSITE MATERIAL OVER THE FREQUENCY RANGE 75 MHz TO 2.0 GHz

Syracuse University

W. F. Walker
Roger E. Heintz

ROME AIR DEVELOPMENT CENTER
Air Force Systems Command
Griffiss Air Force Base, New York 13441

This report has been reviewed by the RADC Public Affairs Office (PA) and is releasable to the National Technical Information Service (NTIS). At NTIS it will be releasable to the general public, including foreign nations.

APPROVED: Roy F. Stratton

ROY F. STRATTON
Project Engineer

APPROVED: David C. Luke

DAVID C. LUKE, Lt Col, USAF
Chief, Reliability & Compatibility Division

FOR THE COMMANDER: John P. Huss

JOHN P. HUSS
Acting Chief, Plans Office

If your address has changed or if you wish to be removed from the RADC mailing list, or if the addressee is no longer employed by your organization, please notify RADC (RBCT), Griffiss AFB NY 13441. This will assist us in maintaining a current mailing list.

Do not return this copy. Retain or destroy.

UNCLASSIFIED

SECURITY CLASSIFICATION OF THIS PAGE (When Data Entered)

REPORT DOCUMENTATION PAGE

READ INSTRUCTIONS BEFORE COMPLETING FORM

1. REPORT NUMBER: RADC-TR-79-255	2. GOVT ACCESSION NO.
3. RECIPIENT'S CATALOG NUMBER	
4. TITLE (and Subtitle): MEASUREMENT OF ELECTRICAL CONDUCTIVITY IN CARBON/EPOXY COMPOSITE MATERIAL OVER THE FREQUENCY RANGE 75 MHz to 2.0 GHz.	5. TYPE OF REPORT & PERIOD COVERED: Phase Report. 1 Oct 77 — 31 Dec 78
	6. PERFORMING ORG. REPORT NUMBER: N/A
7. AUTHOR(s): W. F. Walker, R. E. Heintz	8. CONTRACT OR GRANT NUMBER(s): F30602-76-C-0121, F30602-78-C-0083
9. PERFORMING ORGANIZATION NAME AND ADDRESS: Syracuse University* Syracuse NY 13210	10. PROGRAM ELEMENT, PROJECT, TASK AREA & WORK UNIT NUMBERS: 62702F 233803P2
11. CONTROLLING OFFICE NAME AND ADDRESS: Rome Air Development Center (RBCT) Griffiss AFB NY 13441	12. REPORT DATE: October 1979
	13. NUMBER OF PAGES: 58
14. MONITORING AGENCY NAME & ADDRESS (if different from Controlling Office): Same	15. SECURITY CLASS. (of this report): UNCLASSIFIED
	15a. DECLASSIFICATION DOWNGRADING SCHEDULE: N/A

16. DISTRIBUTION STATEMENT (of this Report)

Approved for public release; distribution unlimited.

17. DISTRIBUTION STATEMENT (of the abstract entered in Block 20, if different from Report)

Same

18. SUPPLEMENTARY NOTES

RADC Project Engineer: Dr. Roy F. Stratton (RBCT)

*The work was done at Rochester Institute of Technology on a subcontract from Syracuse University.

19. KEY WORDS (Continue on reverse side if necessary and identify by block number)

Advanced Composite Materials
Composite Materials
Conductivity
Stripline Method
Electrical Measurements

20. ABSTRACT (Continue on reverse side if necessary and identify by block number)

A stripline technique for the measurement of longitudinal and transverse conductivity of graphite (carbon)/epoxy composite materials over the VHF/UHF (75 MHz to 2.0 GHz) range is described. The method is unusual in that it is essentially free of the uncertain effects of contact resistance between the sample and the measurement apparatus. The underlying theory of the method rests on the relationship between the conductivity of the sample and the lossy standing wave patterns established on the strip transmission line. The method accommodates a range of sample conductivities from 10^2 mhos/m. (Cont'd)

DD FORM 1 JAN 73 1473

UNCLASSIFIED

SECURITY CLASSIFICATION OF THIS PAGE (When Data Entered)

Item 20 (Cont'd)

(e.g. transverse carbon/epoxy) to aluminum (approx. 10^7 mhos/m).

Actual measurements were made from 75 MHz to 2 GHz. The method itself should be usable from 50 MHz to 4 GHz.

ACKNOWLEDGEMENT

In reporting the work performed on this project, it seems most appropriate to acknowledge the contributions of certain individuals not contractually associated with the task, but without whose efforts the work would have been far more difficult.

Professor Walter Gajda of Notre Dame University was patient and helpful in the extreme in obtaining for us the variety of composite material samples tested on the six-foot transmission line. Mr. Kenneth Hood of the Mechanical Engineering Department at RIT provided vital assistance in the design and fabrication of the transmission line test fixture. Mrs. N. Bruening of the RIT EE Dept. was her usual accurate helpful self in the preparation of the final report. Finally, of course, Dr. Roy Stratton of RADC (RBCT) provided knowledgeable guidance throughout the project.

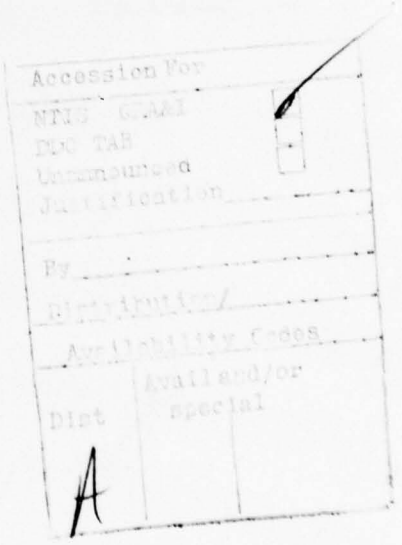

TABLE OF CONTENTS

LIST OF ILLUSTRATIONS

1.0 INTRODUCTION

This is the final report on the development of a technique for the measurement of the admittivity of advanced composite materials (principally graphite/epoxy laminates) in the frequency range of 50 MHz to 4.0 GHz. Measurements reported here cover the range of 75 MHz to 2.0 GHz.

1.1 Review of the Problem

The advanced composite, fiber/matrix, laminate materials find their principal application in sheet form and, in electrical terms, constitute shells of finite electrical thickness whose admittivities are substantially greater than dielectrics (e.g. fiberglass) but are several orders of magnitude lower than metals (e.g. aluminum). Furthermore, in their typical layup geometry, they may be strongly anisotropic and inhomogeneous because of their fibrous nature.

In the frequency band addressed here (75 MHz to 2.0 GHz) representative samples are sufficiently large so that the interaction of the sample and any electric excitation must be treated on a distributed (i.e. wave phenomenon) basis. The result is that the measurement of admittivity (primarily conductivity) is invariably indirect in the sense that what is actually measured is the excitation signal (E or H wave) perturbed by the presence of the sample and its support. It is these perturbations (reflections or transmissions) which must be interpreted and related to the material parameter under investigation.

In many methods aimed at the measurement of conductivity, a principal source of annoyance and inaccuracy is the spurious contact resistance that may arise at the boundary between the advanced composite sample and the rest of the apparatus. This has been a recurring problem in methods based on direct "current vs. voltage-drop" or in methods based on transmission between two chambers partitioned by a sample sheet. A principal advantage of the method described here is that it largely circumvents this contact resistance problem.

1.2 Outline of Earlier Work

The analytical basis for the slotted-stripline composite material tester has been developed in Appendix 3-A of RADC-TR-78-156, "Electromagnetic Properties of Advanced Composite Materials: Measurement and Modelling", June 1978. At the time of that report, the feasibility of the technique had been shown using an improvised line consisting of a 10-inch section of slotted X-band wave guide as the outer conductor of a distorted coaxial line whose inner conductor consists of a strip of composite material sandwiched against the slot using a dielectric spacer to maintain insulation. Measurements made on a unidirectional sample of graphite/epoxy composite material verified the lossy-transmission-line nature of the device. The standing wave data enabled the evaluation of the real (α) and imaginary (β) parts of the propagation factor (γ) along the line, from which the effective longitudinal conductivity could be calculated.

In this report, a longer six-foot slotted-stripline is described, which enabled measurements of conductivity over the range from 75 MHz to 2.0 GHz. The longer line permitted the establishment of nearly a full cycle of standing wave at the lower frequencies.

1.3 Relationship to Overall RADC Composite Material Study

The work reported here is an extension of one of the several directions for investigation established by RADC report: TR-76-206, "A Technology Plan for Electromagnetic Characteristics of Advanced Composites", July 1976 [1]. This report consisted of a survey of the known electromagnetic characteristics of advanced composites and prescribed a number of recommended studies in the areas of: a) intrinsic electrical properties; b) shielding effectiveness of advanced composites; and c) field analysis method for structures involving advanced composites. See, in particular, paragraph 3.1.2.1 of that report which provided the impetus for the work reported here.

2.0 TECHNICAL DISCUSSION

2.1 Review of the Slotted-Stripline Method

2.1.1 Theory

The basic geometry of the slotted stripline composite material tester is shown in Figure 2-1.

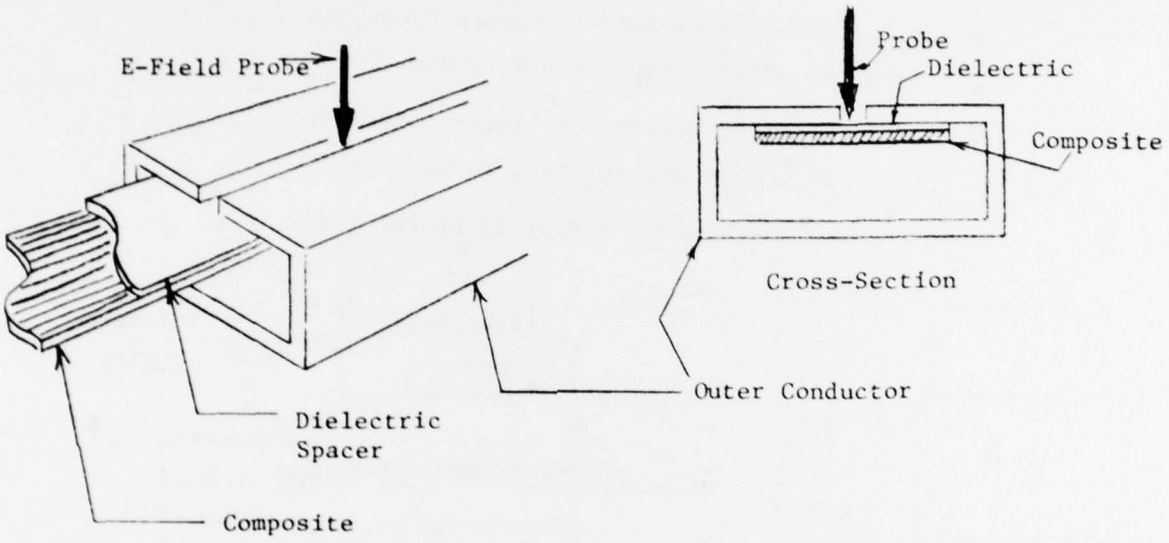

Figure 2-1 SLOTTED STRIPLINE GEOMETRY

The line is driven from an RF source at one end and left "open-circuited" at the other. The finite conductivity of the composite conductor produces a "lossy standing wave pattern" along the line which is sensed by the probe. The E-Field squared-magnitude $|\underline{E}^2|$, is given by:

$$|\underline{E}^2| = K[\cosh(2\alpha x + 2u) + \cos(2\beta x + 2\phi)] \qquad (2\text{-}1)$$

where, K = a "Gain constant" depending upon source strength in $(\text{volts/meter})^2$

x = distance from line end (opposite the source) in meters

α = real part of the propagation factor, γ, in nepers/meter

β = imaginary part of the propagation factor, γ, in radians/meter

u = a "termination factor" in nepers (equal to zero for a pure open circuit termination)

ϕ = a "termination factor, in radians (equal to zero for a pure open circuit termination)

$\gamma = \alpha + j\beta$ = propagation factor along the line.

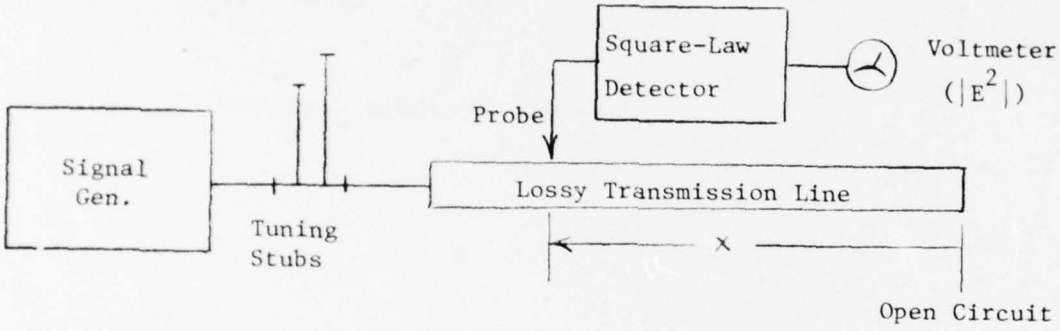

a) Experimental Set-up

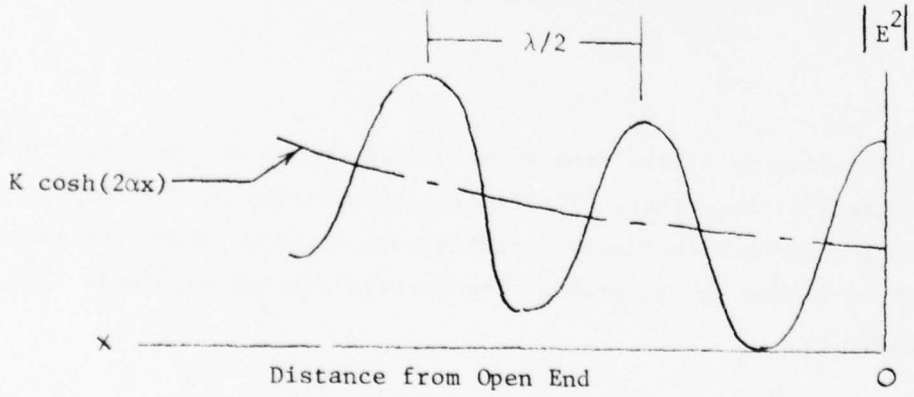

b) Standing Wave Pattern

Figure 2-2 STANDING WAVE MEASUREMENT SET-UP

A schematic representation of the test circuit and a sketch of a typical lossy-line standing wave pattern are given in Figure 2-2.

Reference to the plots of actual data in Appendix A-1 shows good conformity to the typical pattern sketched in Figure 2-2. From the plotted data the real (α) and imaginary (β) parts of the complex propagation factor ($\gamma = \alpha + j\beta$), are readily determined.

In samples of high conductivity along the axis of the line (e.g. aluminum, graphite/epoxy and boron/epoxy with fibers parallel to line axis) the skin depth is small compared to the sample thickness, "a". The admittivity $|\hat{y}|$ of these samples in the direction of propagation along the line is given by [2]:

$$|\hat{y}| \cong \sigma = \frac{\omega\varepsilon_d \beta_o^2}{\{[\alpha^2 - \beta^2 + \beta_o^2]^2 + 4\alpha^2\beta^2\}a^2} \text{ mhos/meter} \quad (2\text{-}2)$$

where,

ω = operating radian frequency

ε_d = permittivity of dielectric spacer

$\beta_o^2 = \omega^2\mu_o\varepsilon_d$

μ_o = permeability of free space = $4\pi \times 10^{-7}$ $\frac{\text{henries}}{\text{meter}}$

α = real part of line propagation constant in nepers/meter

β = imaginary part of line propagation constant in radians/meter

a = thickness of the dielectric spacer in meters

The procedure described above was used in all cases reported here except the case of a graphite/epoxy sample with unidirectional fibers transverse to the direction of propagation along the line. In this case, the transverse conductivity is sufficiently low and the resulting skin depth sufficiently deep to permit the assumption of uniform current distribution over the cross-section of the sample. Under these circumstances the line can be modelled as a simple transmission line (see Figure 2-3).

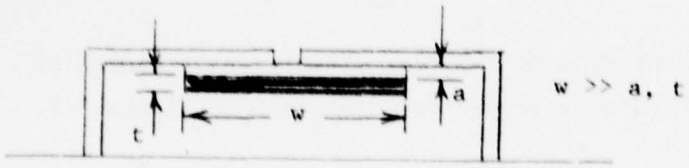

a) Line Cross-Section

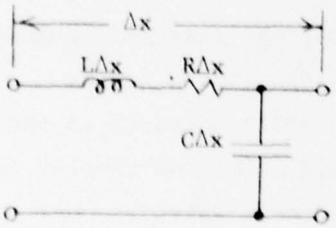

L = inductance/meter

C = capacitance/meter

R = series resistance/meter

b) Differential Line Element

Figure 2-3 LINE MODEL FOR LOW-CONDUCTIVITY SAMPLES

For this model:

$$L \simeq \mu_o \frac{a}{w} \quad \text{henries/meter}$$

$$C \simeq \varepsilon_d \frac{w}{a} \quad \text{farads/meter} \qquad (2\text{-}3)$$

$$R \simeq \frac{1}{\sigma w t} \quad \text{ohms/meter}$$

where a, t, and w are as indicated in Figure 2-3. μ_o and ε_d are the permeability of free space and the permittivity of the dielectric spacer, respectively.

The line impedance z, and admittance y, per unit length, are then,

$$z = R + j\omega L \quad \text{ohms/meter}$$

$$y = j\omega C. \quad \text{mhos/meter} \qquad (2\text{-}4)$$

Accordingly, the propagation factor γ will be:

$$\gamma = \pm \sqrt{zy} = \sqrt{(R + j\omega L)(j\omega C)}$$

$$\cong \sqrt{j\omega RC} = \pm (1 + j) \sqrt{\omega RC/2} \quad \text{for } R >> \omega L \tag{2-5}$$

and

$$\alpha \cong \sqrt{\omega RC/2} \tag{2-6}$$

or

$$2\alpha^2 \cong \omega RC$$

Equations (2-6) and (2-3) can then be used to relate the attenuation constant α to the sample conductivity σ, giving,

$$\sigma \cong \frac{\omega \varepsilon_d}{2\alpha^2 ta} \tag{2-7}$$

For this case, only the attenuation constant need be evaluated from the standing wave data.

2.1.2 Advantages and Limitation of the Method

The method described here has a number of attractive features, as well as a few limitations which should be noted.

Assets:

1 - The method is relatively free of contact resistance problems since poor contact at the drive end of the line only affects the output level - but not the relative standing wave pattern upon which the measurements are based.

2 - Except for the desirability of tuning the probe detector, the method is applicable over an extremely broad band of frequencies ($\simeq$ 1-1/2 decades in this report). For a given line length and cross-sectional geometry, the lower frequency limit is set by the requirement that at least one full cycle of standing wave pattern is

required to provide reasonable estimates of α and β. The upper frequency limit is set up by the line cross-section (see Figures (2-2 and 2-3). At frequencies where the circumferential distances around the sample but inside the outer conductor approach one wavelength, higher modes may be expected which would disturb the pattern. The useable frequency range (as a ratio) could then be expressed as

$$\frac{f_h}{f_L} \simeq \frac{\text{(mean diameter of line)}}{\text{(length)}} . \qquad (2\text{-}8)$$

From this it can be seen that frequency spans well in excess of a decade are readily attainable.

3 - The method is applicable over a span of many decades of values of conductivity σ. As reported here, measured values of conductivity between 10^1 and 10^7 have been made with the method.

4 - Sample sizes required are consistent with normal fabrication methods for composite materials in sheet form.

5 - The instrumentation (in addition to the slotted stripline itself) is commonplace and can be found in the most modestly equipped RF laboratories.

6 - The system is well suited to measuring both transverse and longitudinal components of conductivity in unidirectional composite material samples.

Limitations

In some applications, the method may be seen as having some limitations.

1 - At extremely high frequencies, (e.g., above approximately 5.0 GHz) size and line cross-section required to avoid higher modes will make the analytical model (i.e. a stripline of anisotropic but homogeneous materials) questionable.

2 - The method is not suited to obtaining "bulk" conductivity figures for multi-ply cross-laminated samples.

3 - A certain minimum level of mechanical precision is required both in the construction of the test line and in the formation of test samples. This level of precision is essentially the same as that required of any "slotted-line" type of RF transmission line or waveguide measuring equipment. The irregularities in the standing wave patterns shown in the Appendix are directly attributable to the use of standard extruded aluminum stock (with no surface machining in the construction of the line). Readily discerned mechanical variations in line cross-section corresponded directly to perturbations in the standing wave pattern away from the classic lossy-line form.

2.1.3 Computer Processing of Measured Data

In RADC TR-78-156 (Appendix 3-B) a computer-assisted method was described which was intended to operate on the recorded standing wave data taken from the slotted-stripline measurements and make a "minimum-mean-squared-error" fit of equation (2-1) above, to the data by adjustment of the parameters α, β, u, and ϕ from that equation. This process would then have produced a "best" estimate of the propagation factor components from which the conductivity could be evaluated using equation (2-2). This approach is most useful at low frequencies where only one cycle of standing wave data may be available. With several cycles of data, however, the error function to be minimized has many stationary points (in α, β, u, ϕ - space) and the minimization process (essentially that of "steepest descent") may produce false values. The elaboration of the program in order to deal with this problem was felt to be

of questionable value. At frequencies where two or more cycles of standing wave data can be obtained, the estimation of α and β is sufficiently easy by a graphical inspection of the plotted data, so that recourse to computer analysis is felt to be an unnecessary refinement.

In section 2.3 of this report, the full process of conductivity evaluation is given for representative data, and will be seen to involve, at worst, the solution of a transcendental equation of the form:

$$\cosh y = x, \tag{2-9}$$

by hand calculation. Programmable hand-held calculators of the TI-58, HP-25 or HP-29 type are fully adequate for the task of data reduction.

2.2 Detailed Description of the "6-foot" Slotted Line

2.2.1 The Basic Line

The end view of the 6-foot slotted line (without sample) is shown in Figure 2-4.

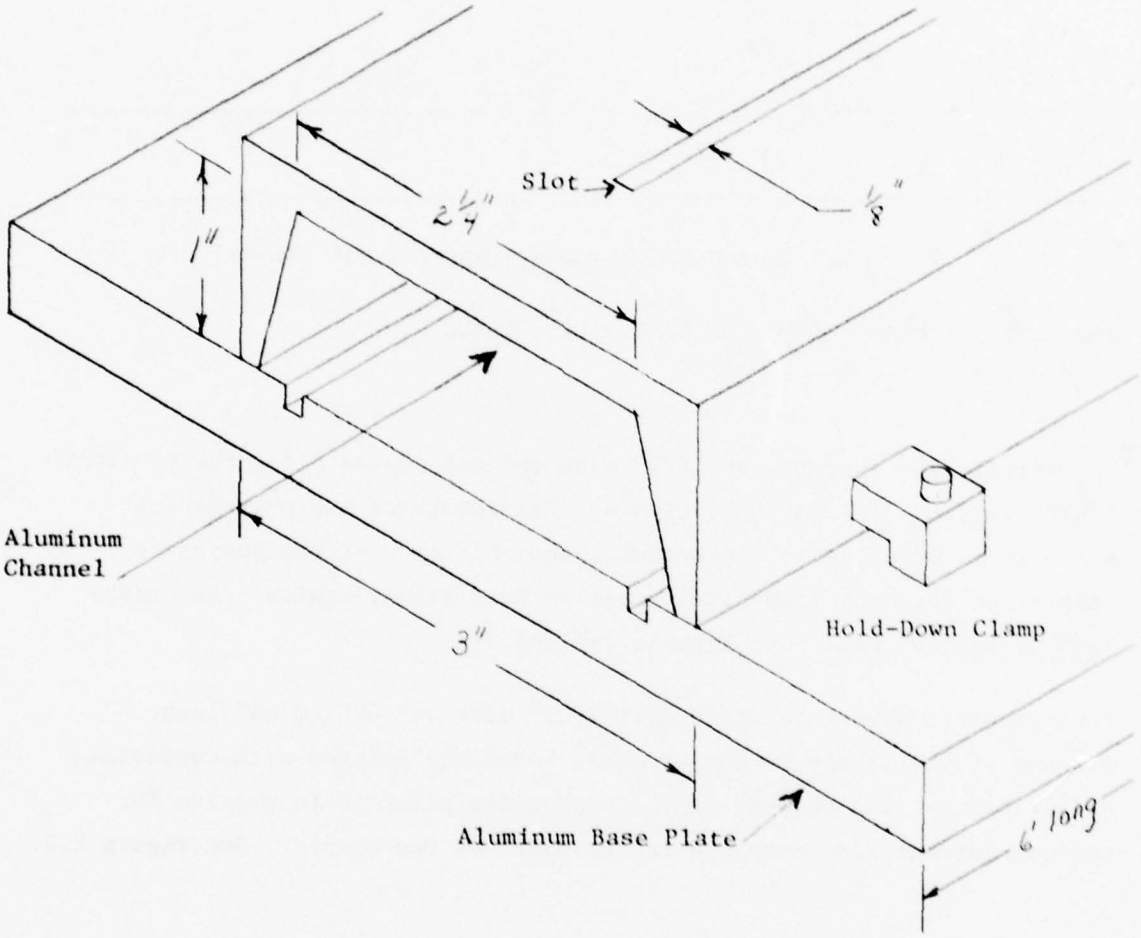

Figure 2-4 END VIEW OF THE 6' SLOTTED LINE

A cross-section of the slotted line, with sample mounted is shown in Figure 2-5.

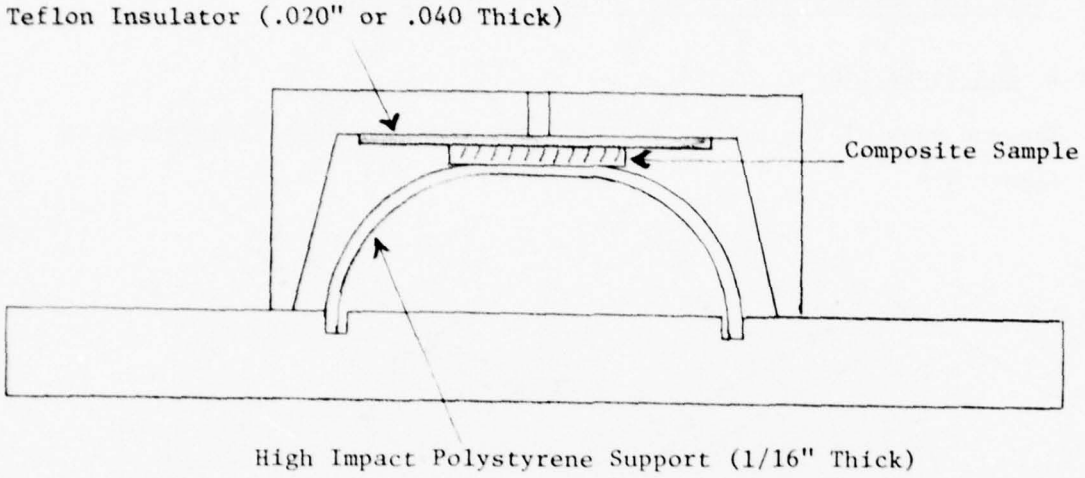

Figure 2-5 CROSS-SECTION OF LINE, WITH SAMPLE

The polystyrene supports are 1/2" wide and are spaced along the 6' length of the slotted line at 2" intervals. The length of the polystyrene supports is adjusted to accommodate, the thickness of the composite sample, so that the composite sample is held firmly against the underside of the channel. See Figures 2-6 and 2-7.

The composite sample is approximately 1" wide and 60" to 66" long. One end of the sample is cut at a 45^{o} bevel and painted with conducting silver paint. The purpose of the conducting paint is to provide for uniform current flow over the entire width of the sample. See Figure 2.8.

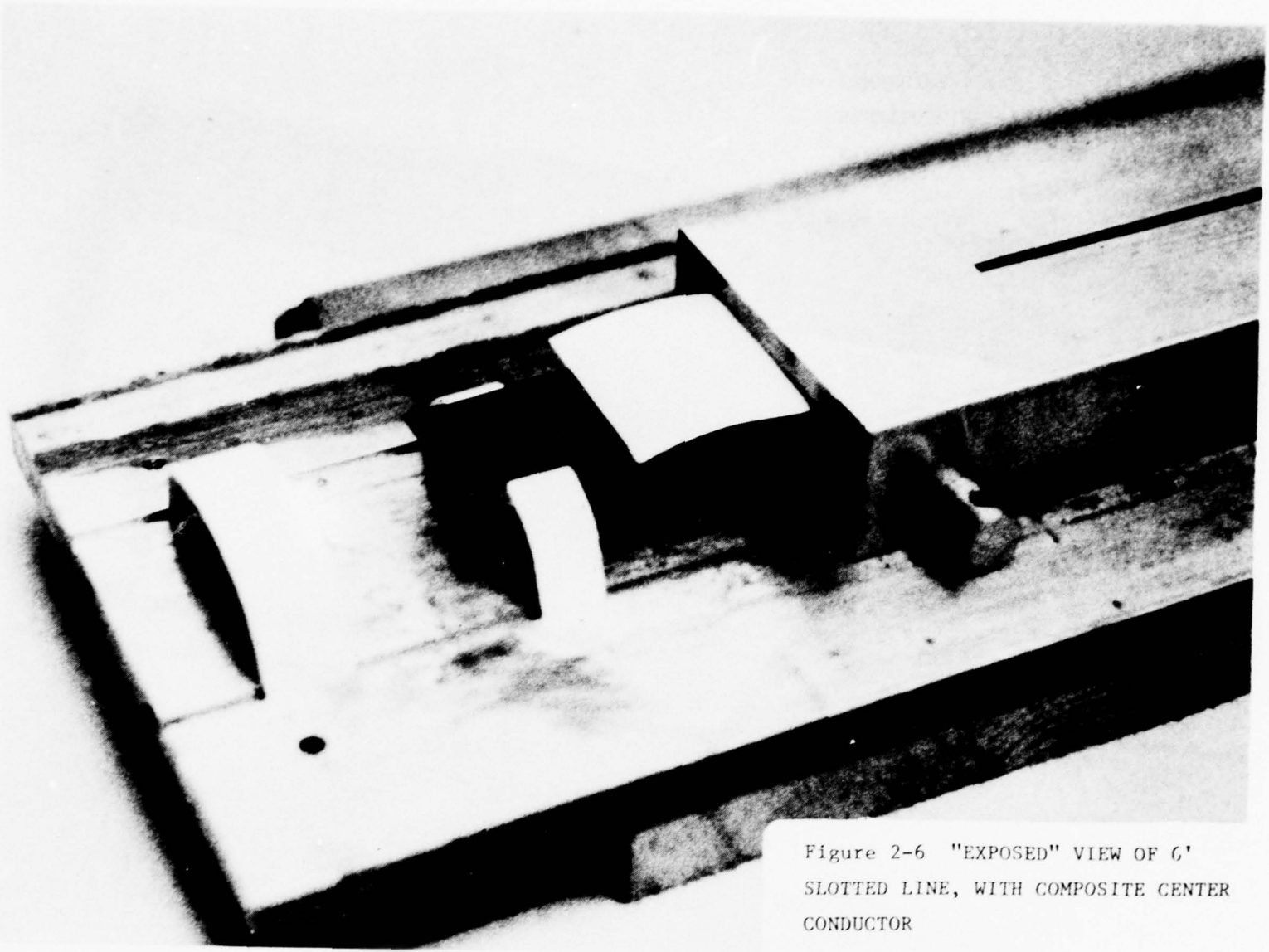

Figure 2-6 "EXPOSED" VIEW OF 6' SLOTTED LINE, WITH COMPOSITE CENTER CONDUCTOR

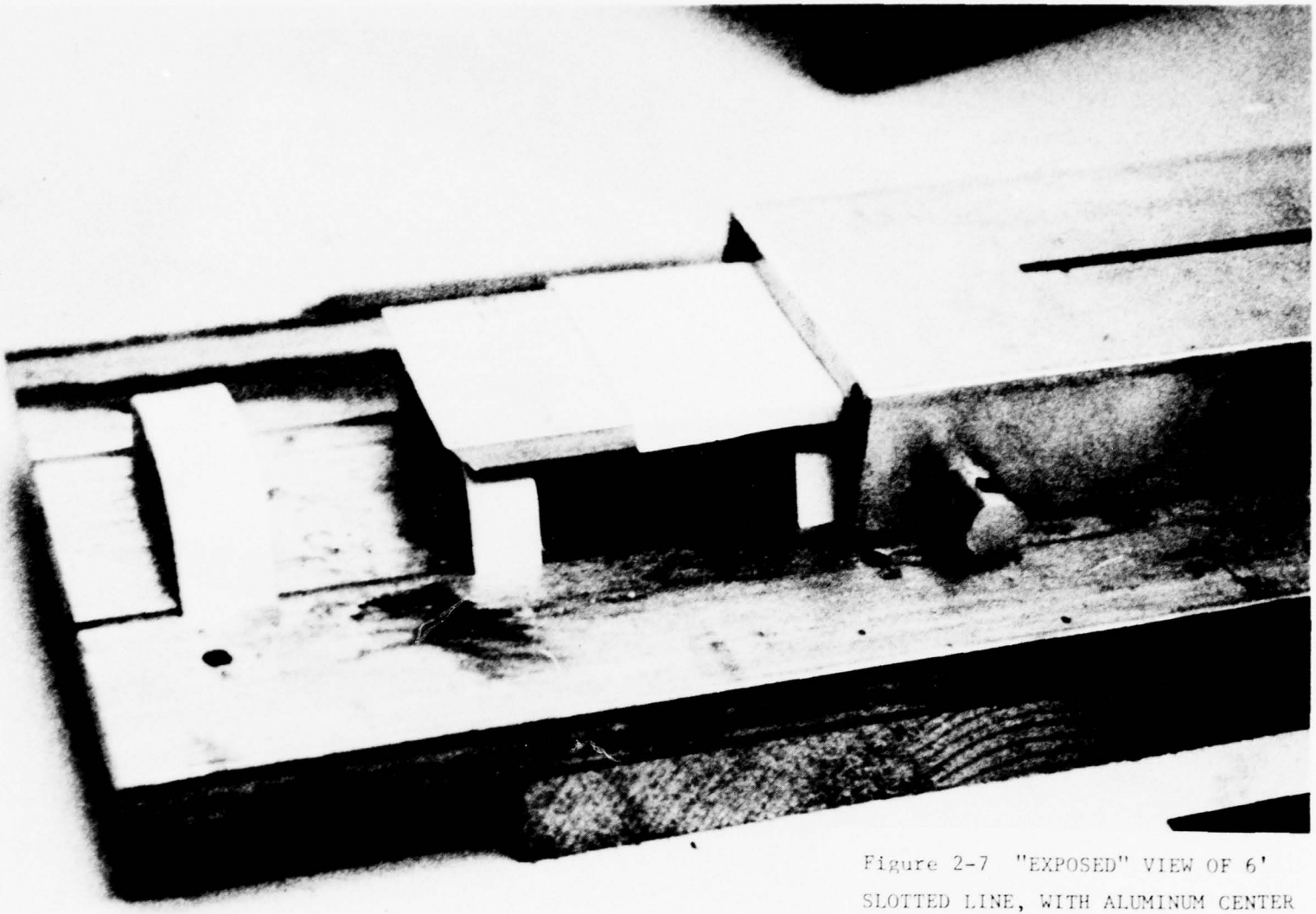

Figure 2-7 "EXPOSED" VIEW OF 6' SLOTTED LINE, WITH ALUMINUM CENTER CONDUCTOR

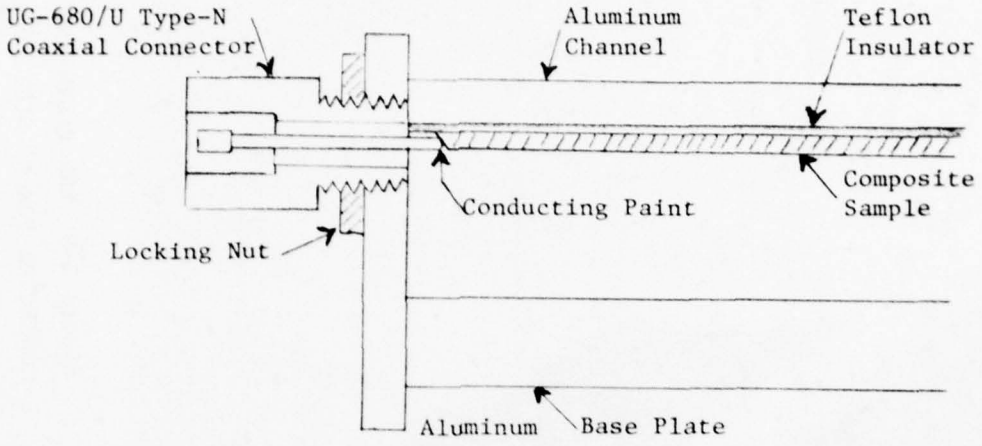

Figure 2-8 "FEED"- END OF 6' SLOTTED LINE
(Sectioned-side view)

A modified UG-680/U type-N coaxial connector is used to connect the high-frequency power source to the composite sample. The coaxial connector is threaded into an end plate which is bolted to one end of the slotted line. See Figure 2-9.

The 10" long slotted line, referred to in section 1.2, is shown in Figure 2-10.

2.2.2 Drive Circuit

A block diagram of the drive circuit is shown in Figure 2-11.

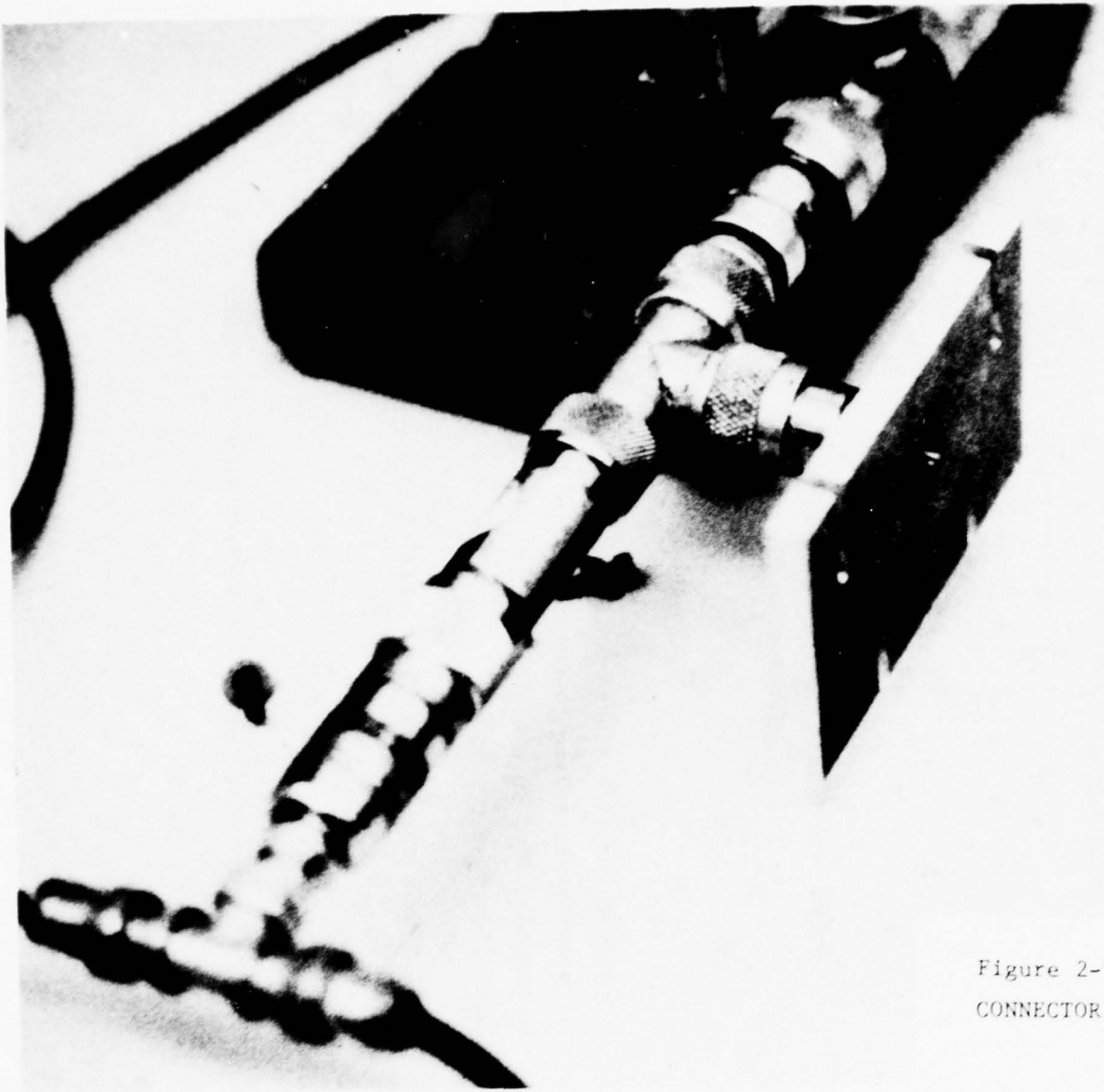

Figure 2-9 END PLATE AND COAXIAL CONNECTOR FOR 6' SLOTTED LINE

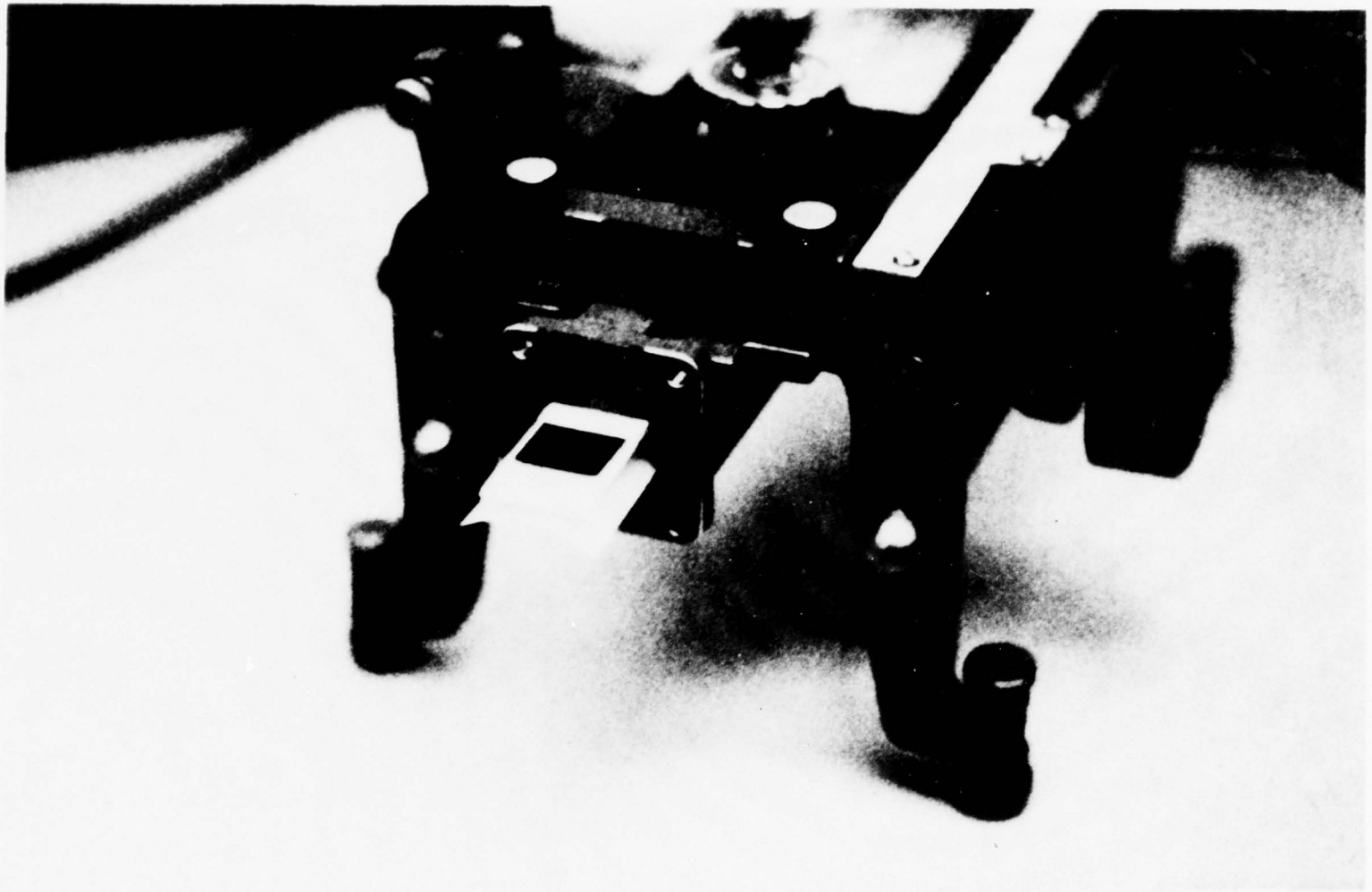

Figure 2-10 "EXPOSED" VIEW OF 10" SLOTTED LINE, WITH COMPOSITE SAMPLE

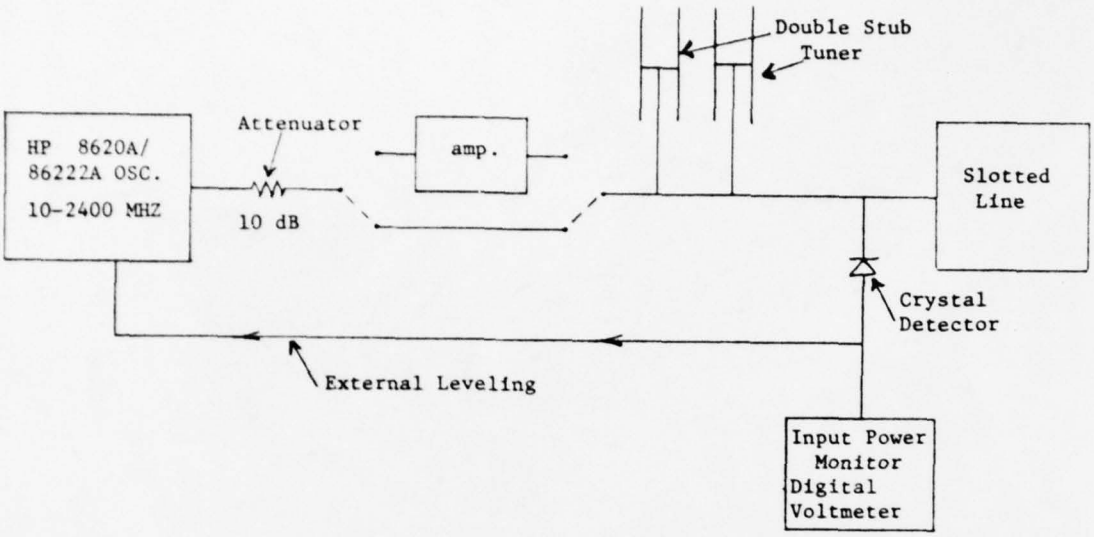

Figure 2-11 BLOCK DIAGRAM OF DRIVE CIRCUIT

The double stub tuner is adjusted (with the external leveling deactivated) to maximize the response at the probe on the slotted line. The oscillator power level is adjusted (with external leveling connected) to the desired level. A high-frequency broadband amplifier may be used to increase the power to the slotted line.

2.2.3 The Probe and Probe Circuitry

The probe circuit is shown in Figure 2-12.

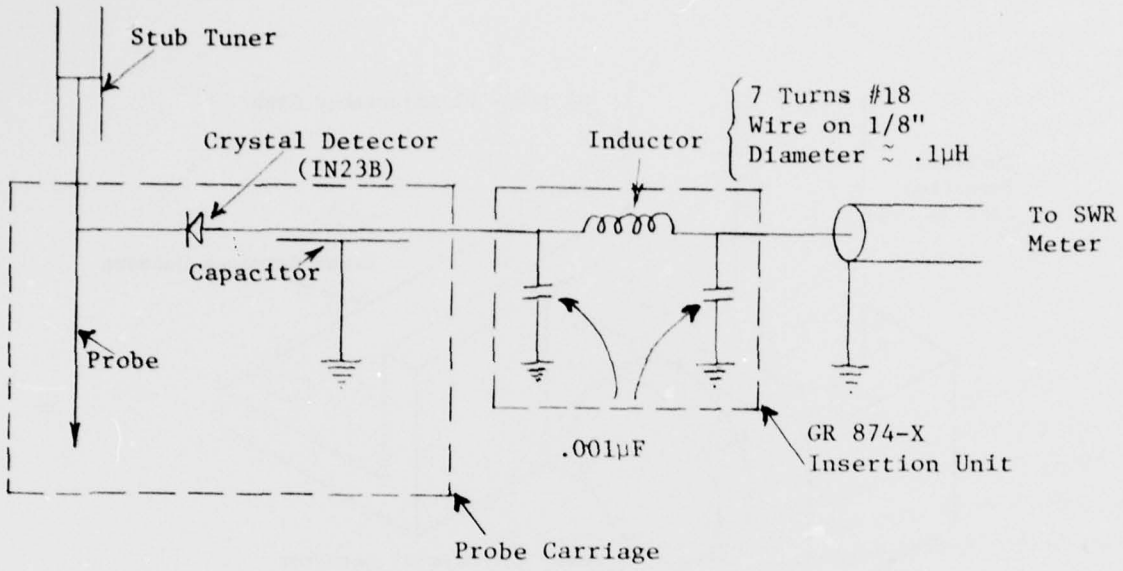

Figure 2-12 PROBE CIRCUIT

Many of the small parts of the probe (carriage) were "borrowed" from the probe carriage of a General Radio 874-LBA coaxial slotted line. A probe body was designed to use these "borrowed" General Radio parts. The depth of penetration of the probe is adjustable. The entire probe carriage rides on top of the aluminum channel on 4 teflon guiding and load-bearing "buttons". Figure 2-13 shows the probe carriage, insertion unit, and tuning stub.

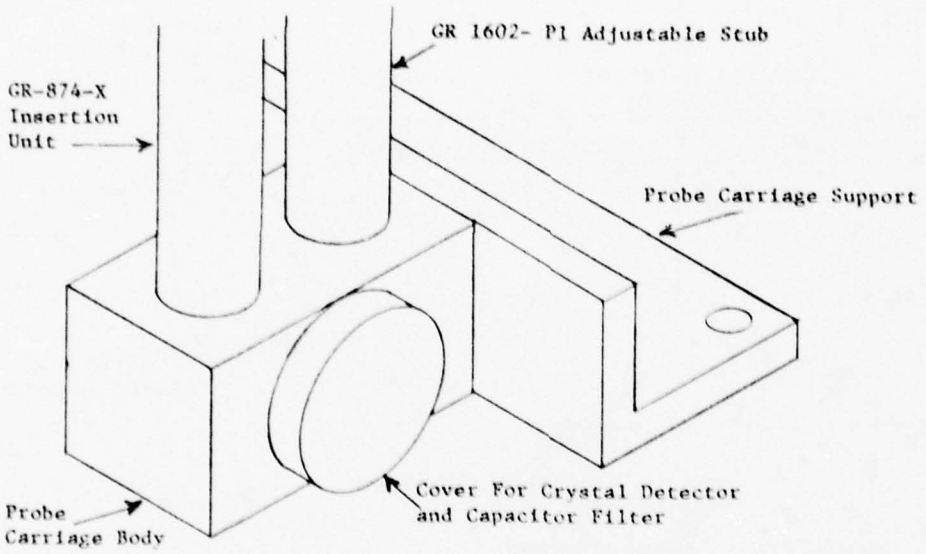

Figure 2-13 PROBE CARRIAGE, INSERTION UNIT, AND STUB TUNER

See also Figures 2-15, 2-16, and 2-17.

2.2.4 Instrumentation and Data Collection

A block diagram of the instrumentation is shown in Figure 2-14.

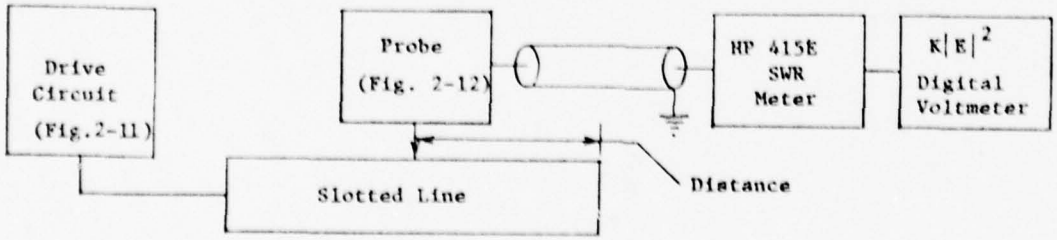

Figure 2-14 BLOCK DIAGRAM OF INSTRUMENTATION

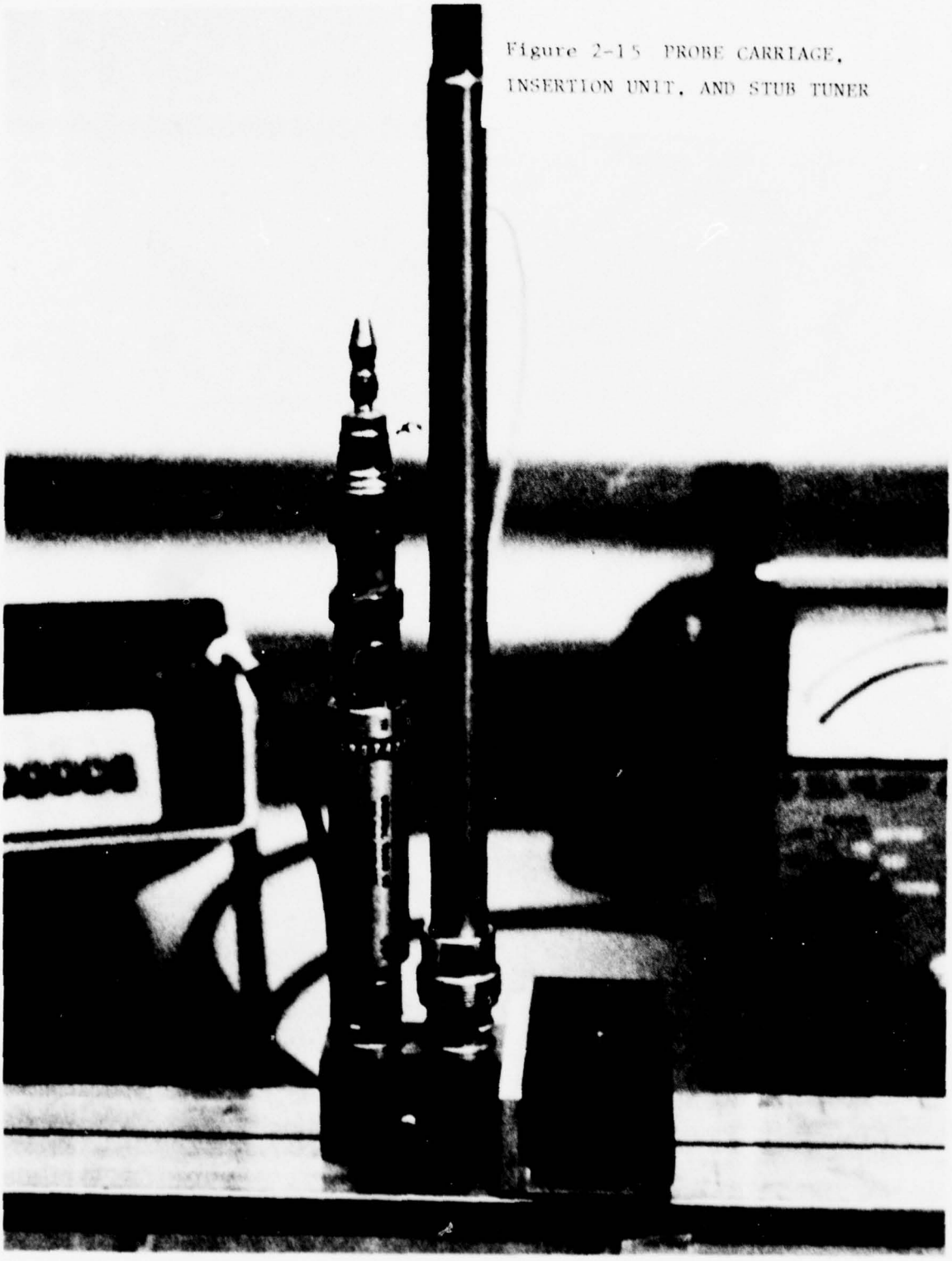

Figure 2-15 PROBE CARRIAGE, INSERTION UNIT, AND STUB TUNER

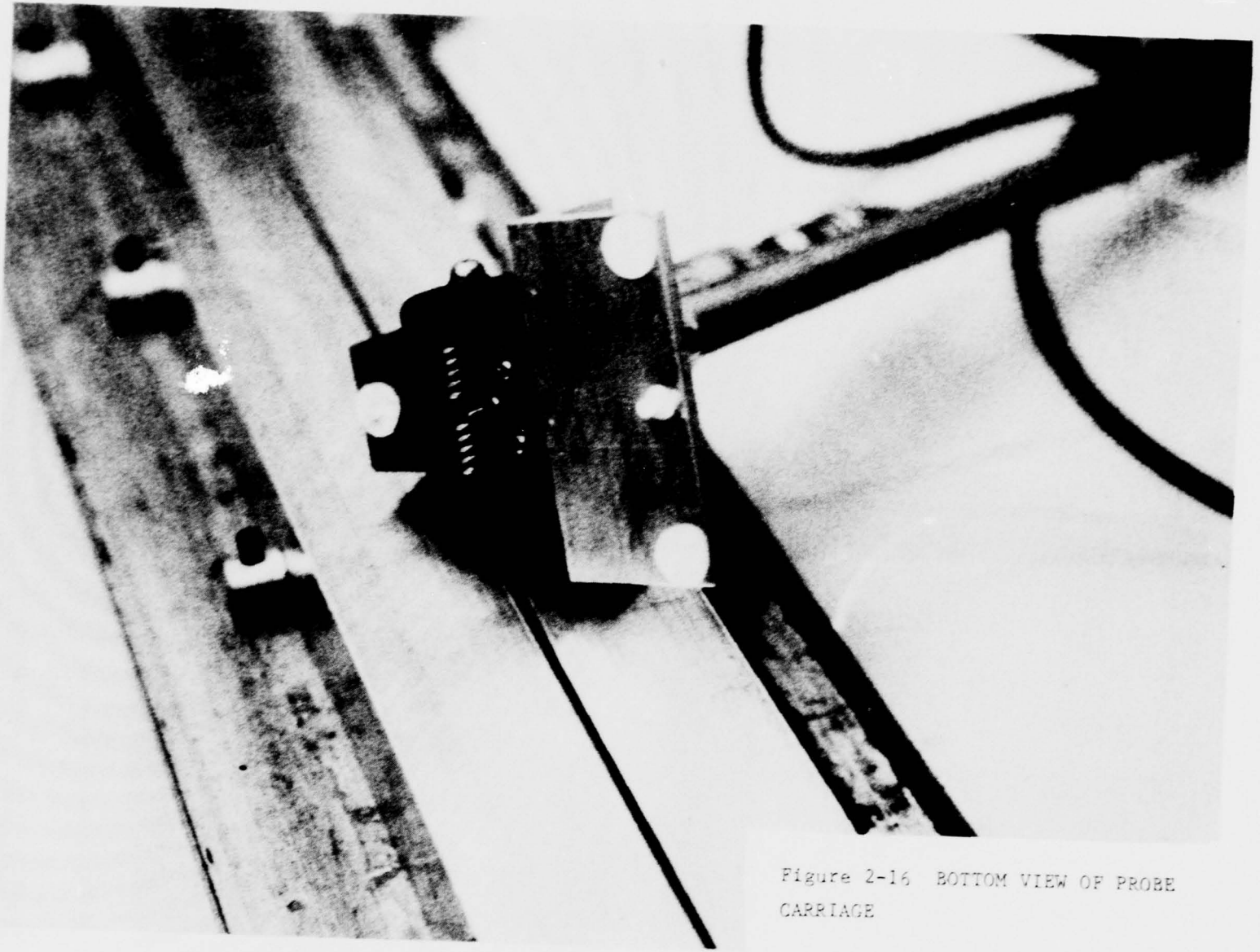

Figure 2-16 BOTTOM VIEW OF PROBE CARRIAGE

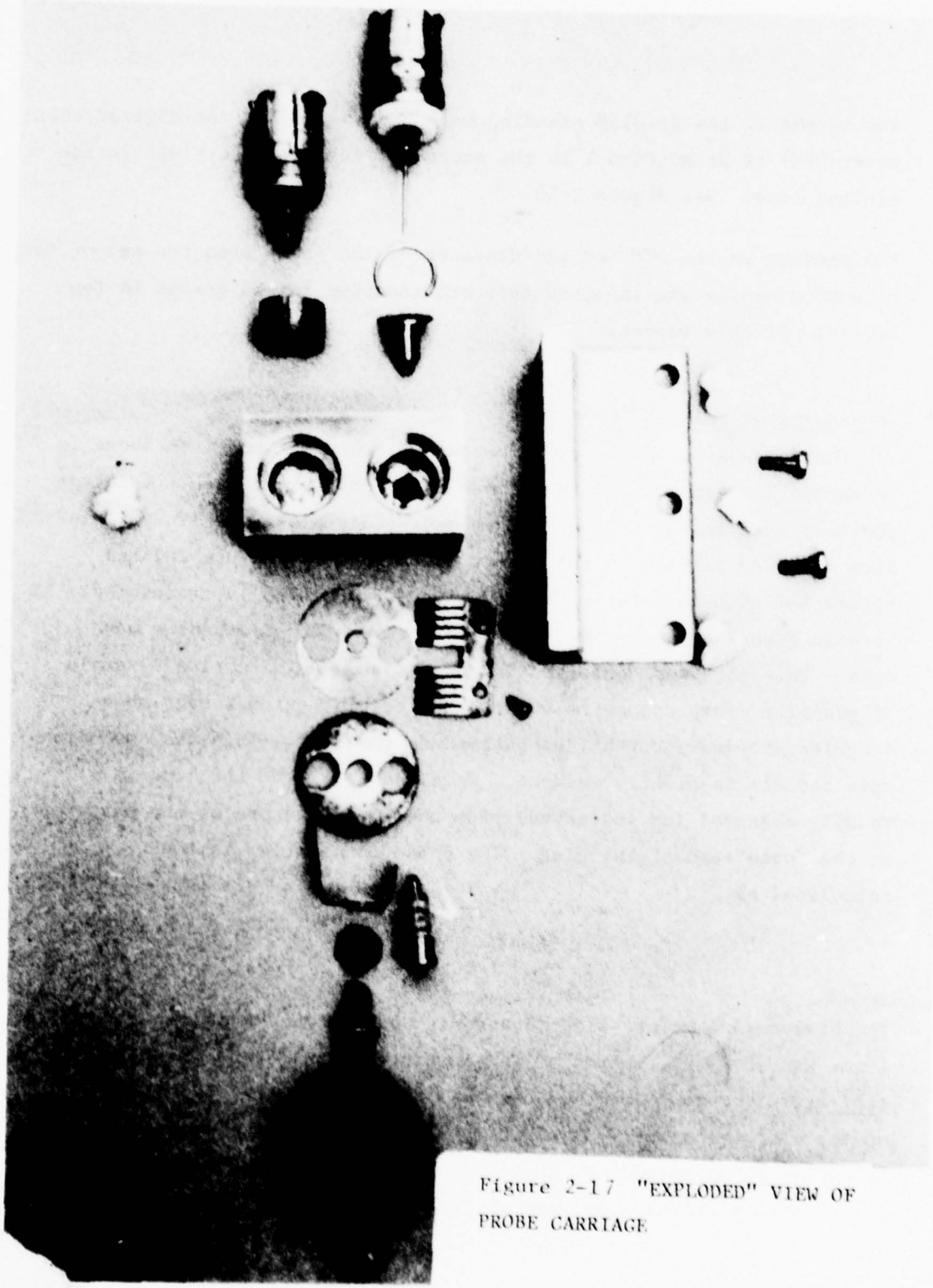

Figure 2-17 "EXPLODED" VIEW OF PROBE CARRIAGE

The output of the HP 415E standing wave indicator (and the digital voltmeter-DVM) is proportional to the square of the electric field in the slotted line. See Figure 2-18.

The reading on the DVM and the distance of the probe from the end of the composite sample are the data that are recorded on the graphs in the appendix of this report.

2.2.5 Processing of STANDING Wave Data

The discussion of the experimental instrumentation given above in paragraph 2.2.4 described the manner in which the square-law detector provided data in the form of $K|\underline{E}^2|$ vs distance along the line. This data was then plotted in the manner illustrated by Figure 2-2 and Figure A-1 through A-14 in the Appendix. Figure A-3 is reproduced here as Figure 2-19 to show a representative plot of standing wave data. This data was collected at 300 MHz on a unidirectional sample of graphite/epoxy composite material. The plot extends over about 4 cycles (two wavelengths) of pattern on the line. The lossy standing-wave pattern is clearly evident. Wavelength, λ_g, on the line is readily measured (as indicated) from the cyclic nature of the pattern at the "open" end of the plot. The phase constant β_g is then calculated as:

$$\beta_g = \frac{2\pi}{\lambda_g} \quad .$$

The broken line on the plot represents the sketched estimate of the term, K cosh $(2\alpha y)$, where "y" is the distance in meters toward the generator from the "open circuit" end of the line (157 centimeters on the distance scale). Two widely separated points on this broken line can be used to solve for the gain constant K and the attenuation constant α as follows (see Figure 2-19):

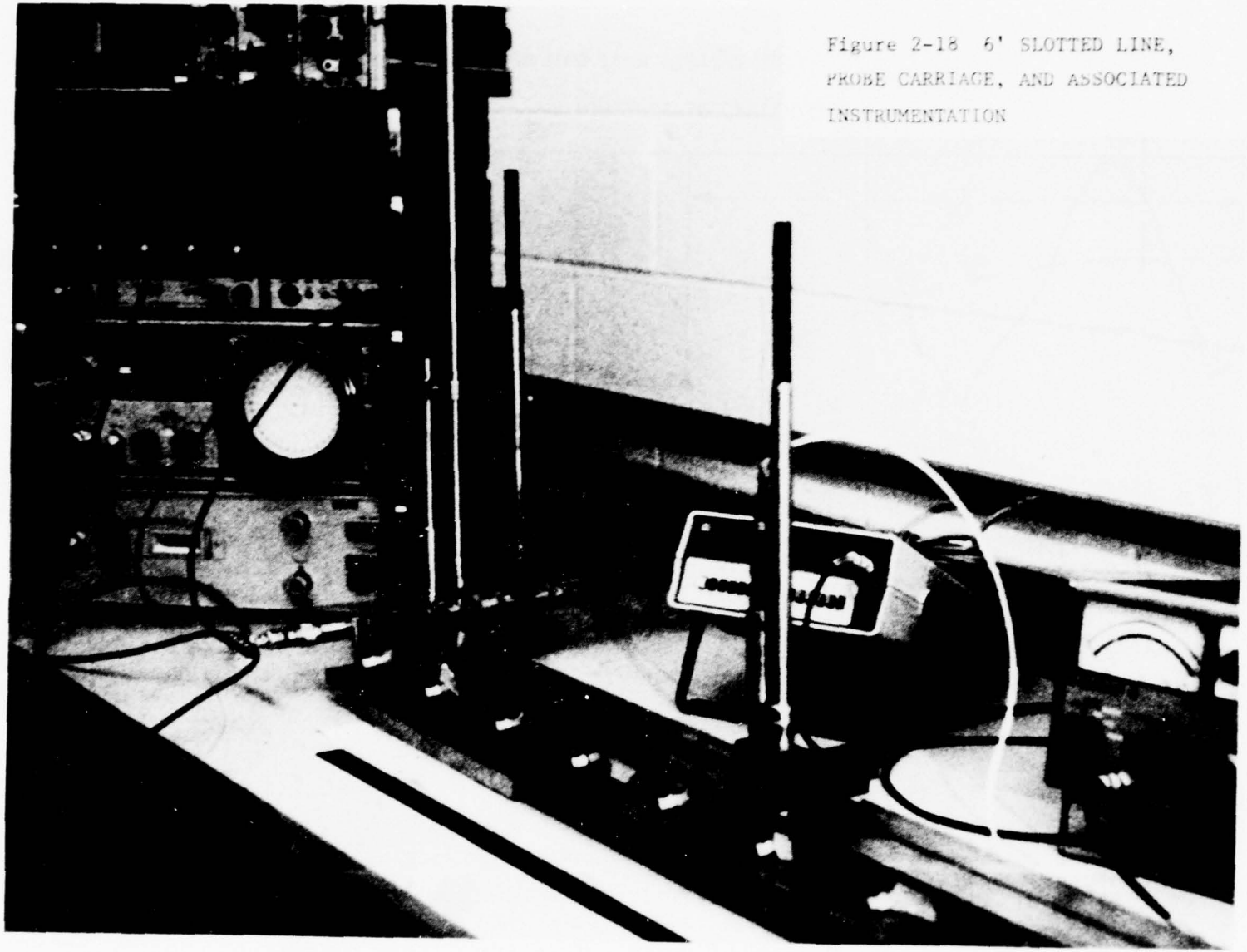

Figure 2-18 6' SLOTTED LINE, PROBE CARRIAGE, AND ASSOCIATED INSTRUMENTATION

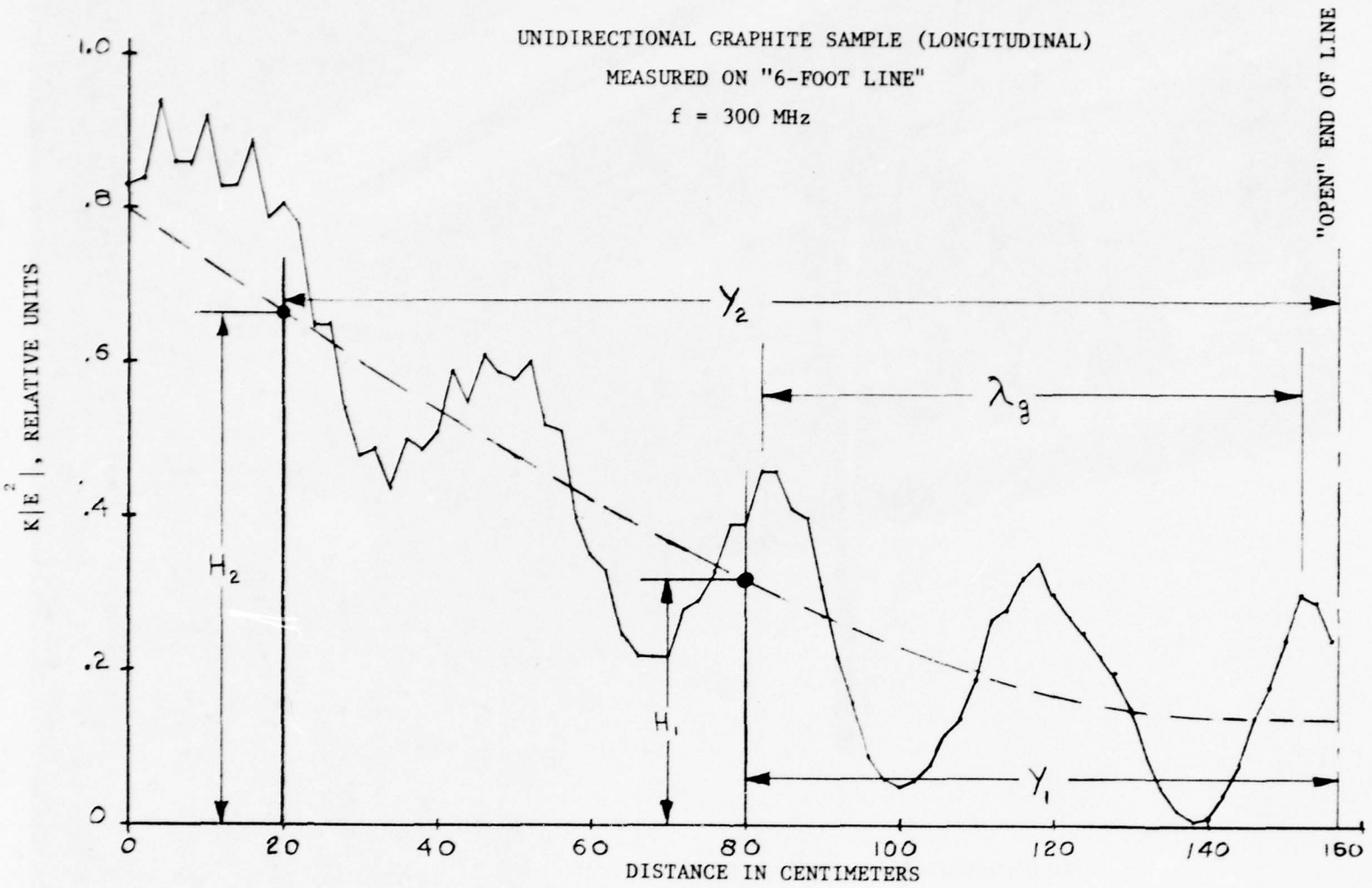

FIGURE 2-19 PARAMETER ESTIMATION FROM PLOTTED DATA

we have,

$$H_1 \cong K \cosh(2\alpha y_1)$$

$$H_2 \cong K \cosh(2\alpha y_2) \quad .$$

Then

$$\cosh(2\alpha y_2) = \left(\frac{H_1}{H_2}\right) \cosh(2\alpha y_1) \quad .$$

This last transcendental equation is then solved iteratively on a pocket calculator to yield α. The conductivity, σ, is then evaluated according to equation (2-2), given previously. In the case of Figure 2-19), the results were:

$$\beta_g \cong 8.89 \text{ radians/meter}$$

$$\alpha \cong .80 \text{ nepers/meter}$$

$$\sigma \cong 5.03 \times 10^4 \text{ mhos/meter.}$$

2.3 Measured Results

2.3.1 Graphite/Epoxy (Longitudinal)

Figures A-1 through A-11 show plotted data taken on the six-foot slotted line on a unidirectional graphite/epoxy sample (fibers parallel to propagation direction) over the range from 75 MHz to 2.0 GHz. A plot of measured conductivity versus frequency for this sample is shown in Figure 2-20. The plot shows a gradually decreasing conductivity with increasing frequency for which no explanation seems currently available.

2.3.2 Aluminum

Figures A-12 and A-13 in the Appendix show standing-wave data taken on an aluminum strip in place of the composite strip. These plots serve two useful functions. Firstly, they confirm the validity of the basic method by means of their much "deeper" standing wave trough

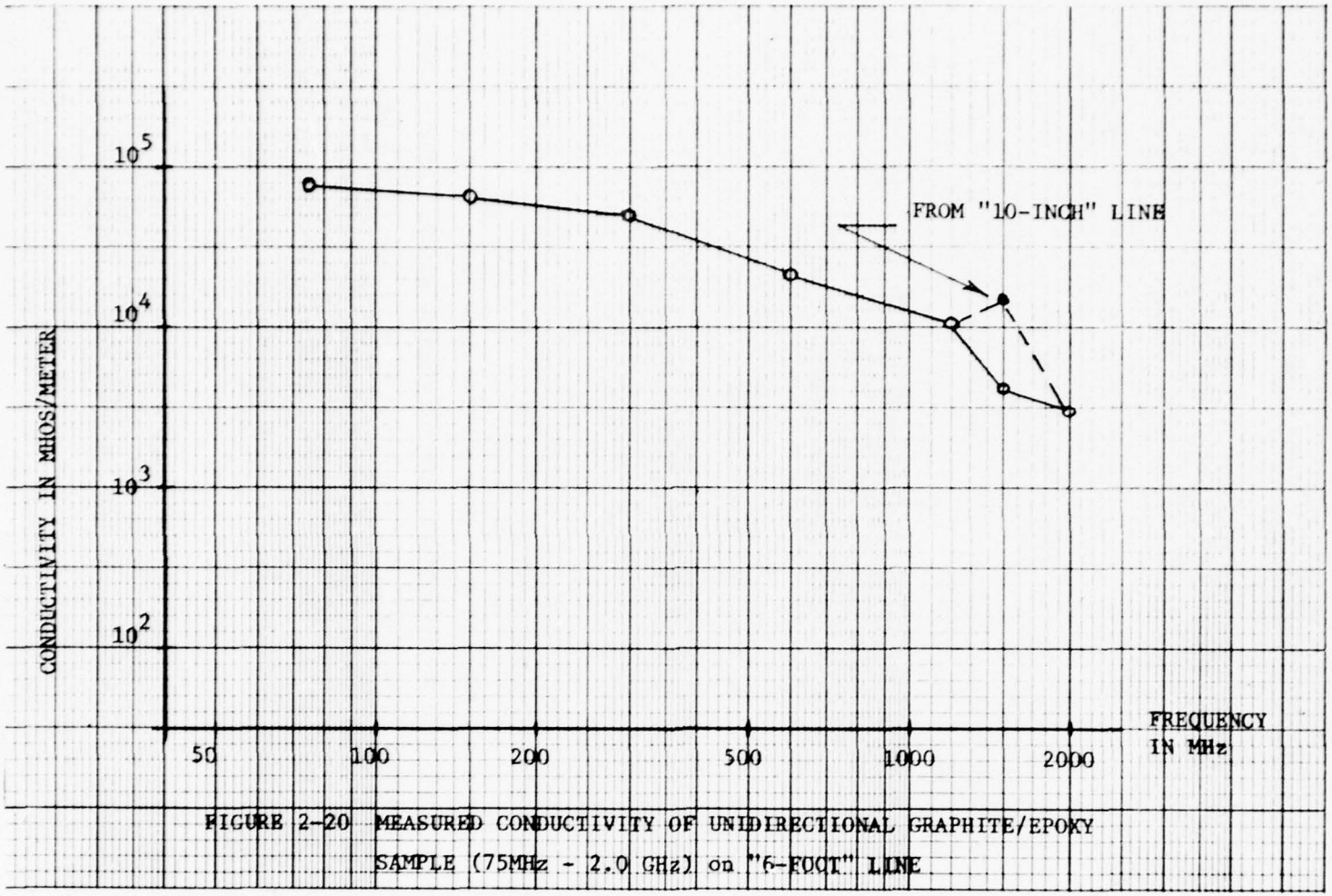

FIGURE 2-20 MEASURED CONDUCTIVITY OF UNIDIRECTIONAL GRAPHITE/EPOXY SAMPLE (75MHz - 2.0 GHz) on "6-FOOT" LINE

all along the line as compared with those of the graphite sample at the same frequencies. These trough depths indicate a conductivity of the order of $\sigma \simeq 10^7$ for aluminum. Secondly, the irregularity in the standing wave peaks (higher peaks in the 0.3 to 0.8 meter portion of the distance scale) suggested a lack of uniformity in the cross-sectional dimensions of the line which was later confirmed. A similar "spatial effect" is noticeable in the patterns of Figures A-1, A-3, A-5 and A-7 where a cyclic fluctuation in the pattern is noticeable with a period of about 5 cm. at the left hand end of the plots. This 5 cm. dimension was found to check well with the spacing of the plastic "springs" which held the sample against the slot.

2.3.3. Boron

Figure A-14 shows the standing wave pattern taken on the 10-inch slotted stripline for a sample of boron/epoxy composite. It should be noted that the resulting calculated conductivity of $\sigma \simeq 7 \times 10^4$ mhos/meter is significantly higher than values obtained by other methods, whereas the measured conductivities for the graphite sample are quite consistent with measurements by others (3), (4) at frequencies above and below those reported here.

2.3.4 Transverse Graphite Epoxy

A sample of graphite/epoxy with fibers transverse to the direction of propagation was tested in the 10-inch line at 1.0 GHz. In this case the attenuation was so high that reflected waves were negligible and a direct measurement of "α" was possible on the line. The data was as follows:

a = dielectric spacer thickness = 2.54×10^{-4} meters

t = sample thickness = 6.35×10^{-3} meters

ε_d = Spacer permittivity = 1.95×10^{-11} farads/meter

ω = $2\pi(1.0\ \text{GHz}) = 6.28 \times 10^9$ radians/second

α = 69.3 nepers/meter.

The result as given by equation (2-7) was:

$$\sigma \simeq \frac{\omega\varepsilon_d}{2\alpha^2 ta} = 7.91 \text{ mhos/meter .}$$

As a check, the measurement was repeated after increasing the dielectric spacer thickness by a factor of 4 to 1.02×10^{-3} meters. The data in this case was:

$$a = 1.02 \times 10^{-3} \text{ meters}$$
$$t = 6.35 \times 10^{-3} \text{ meters}$$
$$\varepsilon_d = 1.95 \times 10^{-11} \text{ farad/meter}$$
$$\omega = 2\pi \times 10^9 \text{ radian/sec.}$$
$$\alpha = 38.8 \text{ nepers/meter.}$$

The result in this case was:

$$\sigma \simeq \frac{\omega\varepsilon_d}{2\alpha^2 ta} = 6.28 \text{ mhos/meter.}$$

The agreement here was good despite the four-to-one change in spacer thickness.

2.4 Summary Discussion of the Method

The work reported here is perhaps best viewed as a fairly thorough demonstration of the feasibility of the slotted stripline method over a broad range of frequencies and sample conductivities. In the process, the measured results gave a clear indication of the areas in which the method could be improved to the level where consistently accurate results could be obtained routinely.

2.4.1 Results on Experimental Lines

The 10-inch Line

This line was effective above 1.0 GHz where at least one full cycle of standing wave pattern was attainable. Furthermore the mechanical precision of the line provided classic lossy-standing-wave patterns at frequencies between 1.0 and 2.0 GHz. (See Figure A-14). The detector probe on this line was untuned, however, which resulted

in considerable loss of sensitivity. This loss was not serious in the case of the highly conductive graphite/epoxy and boron/epoxy longitudinal samples, but prevented extended pattern measurement in the case of the highly lossy transverse graphite/epoxy measurement. Tuning the probe would have greatly increased the detector output and also suppressed harmonics (if present) in the signal generator which could greatly contaminate the standing wave pattern.

Due to the short circumferential distance around the sample strip within this line, it could be used readily up to about 5.0 GHz without danger of higher propagating modes.

The Six-Foot Line

The six-foot line was highly effective from 75 MHz to 2.0 GHz. Its lack of mechanical precision, principally with regard to uniformity of cross-section caused some noticeable perturbation of the standing-wave pattern along the line. Its "carcass", however, was simply a slotted length of stock aluminum channel extrusion. In a line with a more rigid structure, machined with a precision consistent with standard slotted line instruments, these perturbations would not occur.

There still remained some spurious radiation from the slot which interacted with the probe carriage on the six-foot line. It is felt that this interaction could be substantially reduced by a deeper slot into which to the inner and outer (shield) conductors of the probe could extend.

2.4.2 Recommendations for Refinement of the Method

2.4.2.1 Basic Line Cross-Section

A sketch of a proposed improved line cross-section is shown in Figure 2-21. In comparing this with the cross-section of the experimental line, a number of features are worth emphasizing:

a) The entire structure is more rigid. This coupled with machining of the sample bed and probe carriage track will provide the uniformity in cross-section necessary for pure lossy-line standing-wave patterns.

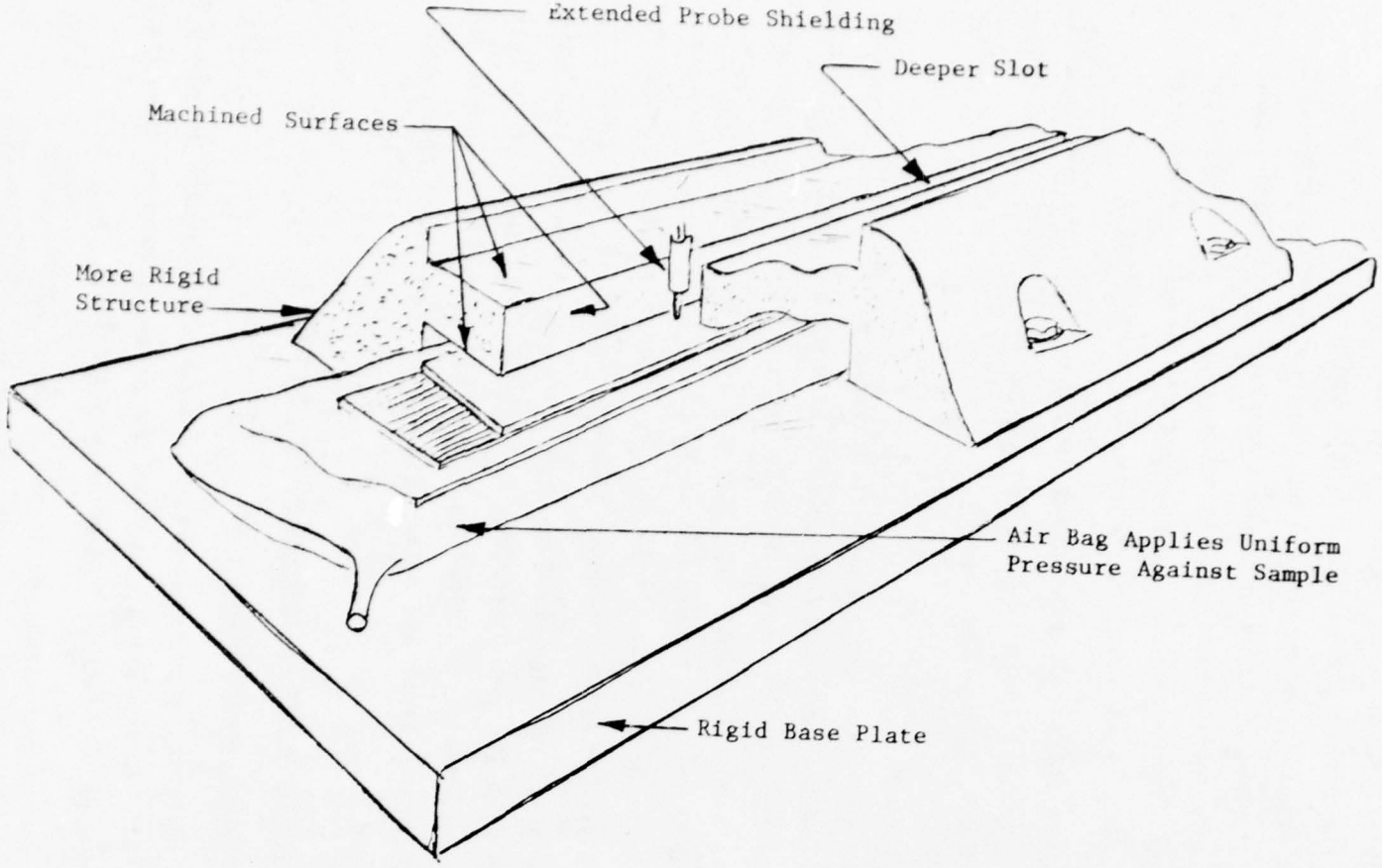

FIGURE 2-21 SKETCH OF IMPROVED LINE STRUCTURE

b) The circumferential distance around the sample strip is reduced allowing for operation at higher frequencies.

c) The slot is considerably deeper to better contain the field and shield the probe.

2.3.2.2 Probe Design

Two improvements are suggested in connection with the probe and its carriage.

a) Take advantage of the shielding features of a deeper slot by carrying both the inner and outer conductors of the probe deeper into the slot. Probe depth adjustment should still be retained, however.

b) In any given band of operation, the tuning circuit for the probe should have a single adjustable resonant peak. Since the system itself is capable of operation over a broad band, this precaution prevents inadvertent tuning to signal harmonics, as is possible with "stub-tuning."

3.0 REFERENCES

(1) A Technology Plan for Electromagnetic Characteristics of Advanced Composites, RADC-TR-76-206, July 1976, A030507.

(2) Electromagnetic Properties and Effects of Advanced Composite Materials: Measurement and Modelling, RADC-TR-78-156, June 1978, A058041.

(3) Electromagnetic Effects of Advanced Composites, C. Skouby, Final Report, (ONR), January 1975, Contract N00014-74-C-0200, McDonnell Aircraft Co.

(4) D. Strawe, L. Piszker, "Electromagnetic Shielding of Advanced Composites in the 10 KHz to 100 MHz Frequency Range", (AFML) Final Report, July 1975 Contract F 33615-74-C-5158, Boeing Aerospace Co.

4.0 APPENDIX - Experimental Data

FIG. A-1 UNIDIRECTIONAL GRAPHITE SAMPLE (LONGITUDINAL)
MEASURED ON "6-FOOT" LINE

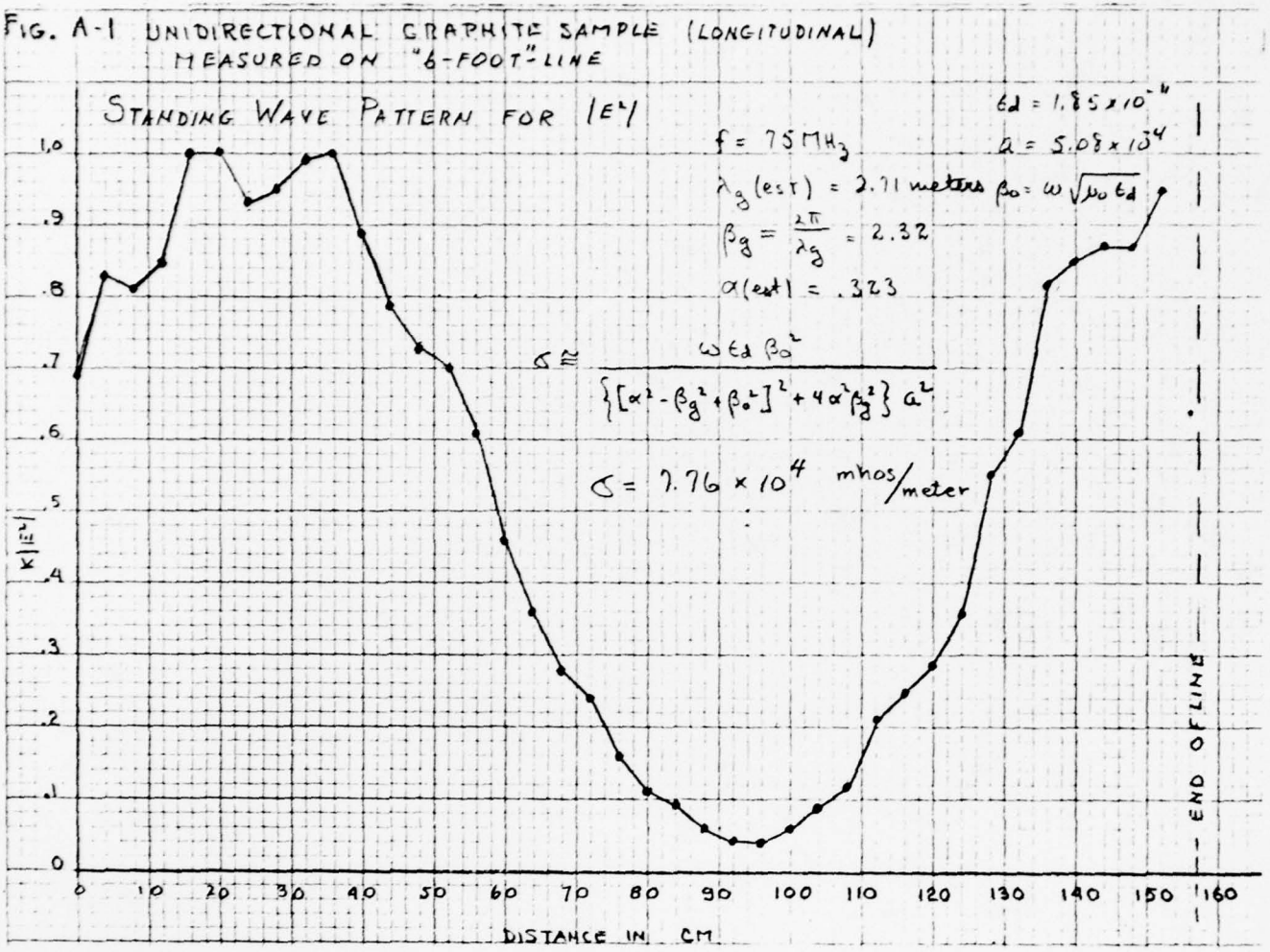

FIG. A-2 UNIDIRECTIONAL GRAPHITE SAMPLE (LONGITUDINAL) MEASURED ON "6-FOOT" LINE

STANDING WAVE PATTERN FOR $|E^2|$

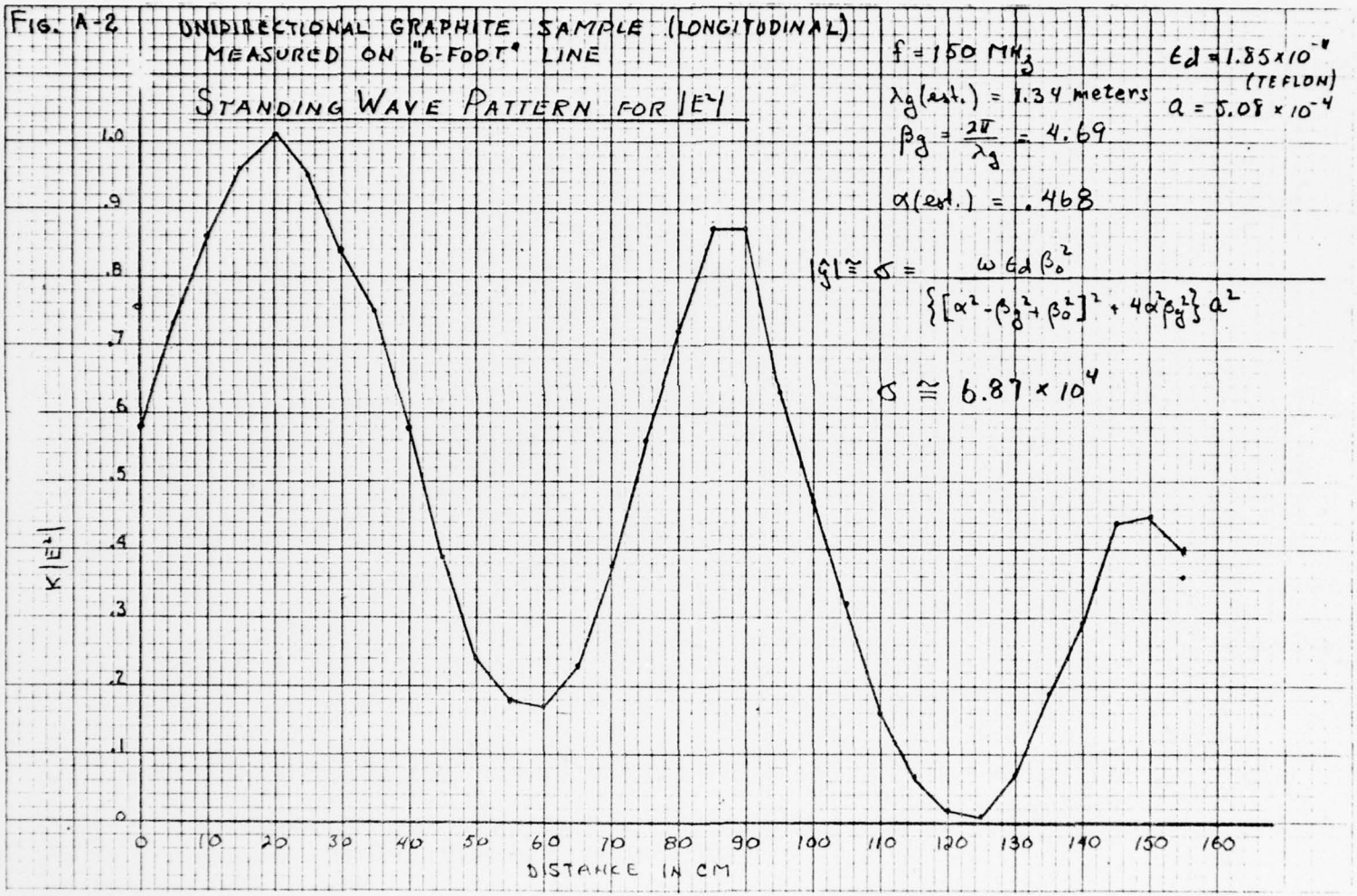

$f = 150$ MHz $\quad \epsilon_d = 1.85 \times 10^{-4}$ (TEFLON)

λ_g(est.) = 1.34 meters $\quad a = 5.08 \times 10^{-4}$

$\beta_g = \frac{2\pi}{\lambda_g} = 4.69$

α(est.) = .468

$$|g| \cong \sigma = \frac{\omega \epsilon_d \beta_o^2}{\left\{\left[\alpha^2 - \beta_g^2 + \beta_o^2\right]^2 + 4\alpha^2\beta_g^2\right\} a^2}$$

$\sigma \cong 6.87 \times 10^4$

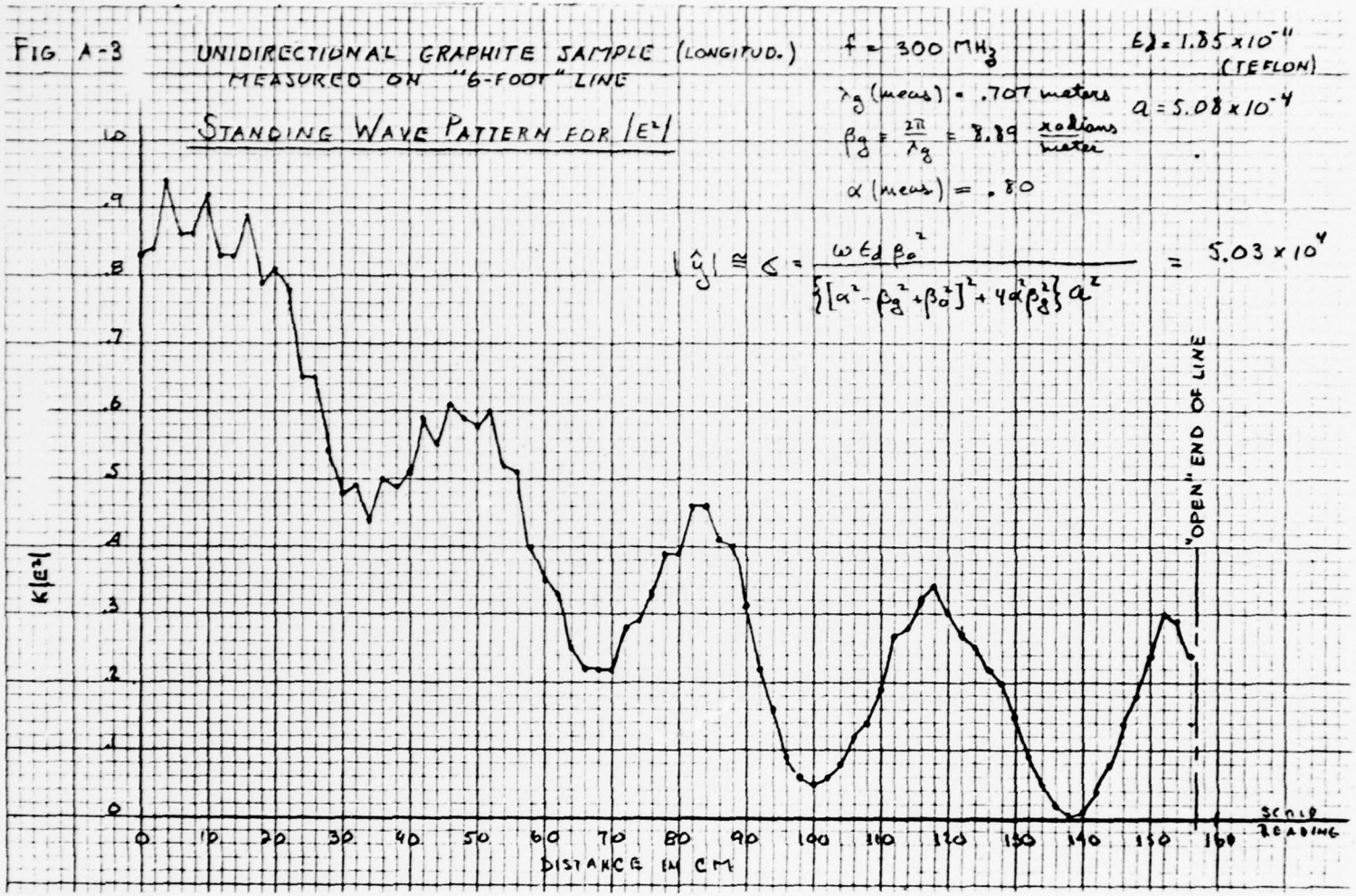
FIG A-3
UNIDIRECTIONAL GRAPHITE SAMPLE (LONGITUD.)
MEASURED ON "6-FOOT" LINE
STANDING WAVE PATTERN FOR |E²|
f = 300 MHz
λg (meas) = .707 meters
βg = 2π/λg = 8.89 radians/meter
α (meas) = .80
εd = 1.85 x 10⁻¹¹ (TEFLON)
a = 5.08 x 10⁻⁴
|ĝ| ≅ δ = ωεd β0² / {[α² - βg² + β0²]² + 4α²βg²} a² = 5.03 x 10⁴
K|E²|
0 .1 .2 .3 .4 .5 .6 .7 .8 .9 1.0
0 10 20 30 40 50 60 70 80 90 100 110 120 130 140 150 160
DISTANCE IN CM
SCALE READING
"OPEN" END OF LINE

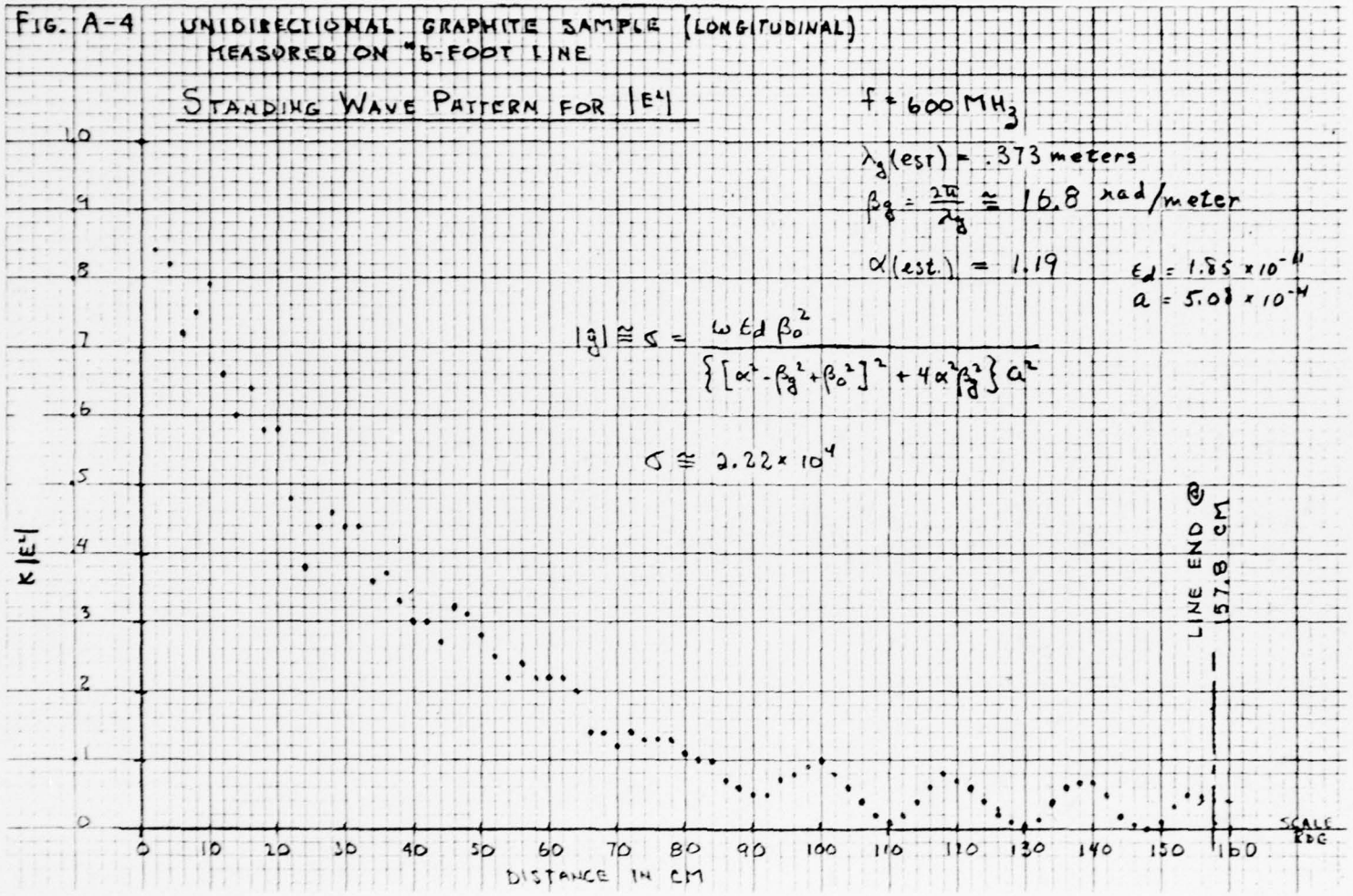
FIG. A-4 UNIDIRECTIONAL GRAPHITE SAMPLE (LONGITUDINAL)
MEASURED ON "5-FOOT LINE
STANDING WAVE PATTERN FOR |E²|
f = 600 MH3
λg (est) = .373 meters
βg = 2π/λg ≅ 16.8 rad/meter
α (est.) = 1.19
εd = 1.85 × 10⁻¹¹
a = 5.08 × 10⁻⁴
|Ĝ| ≅ σ = ωεd β0² / {[α² - βg² + β0²]² + 4α²βg²} a²
σ ≅ 2.22 × 10⁴
K |E²|
LINE END @ 157.8 CM
SCALE EDG
DISTANCE IN CM
0 10 20 30 40 50 60 70 80 90 100 110 120 130 140 150 160
0 1 2 3 4 5 6 7 8 9 10

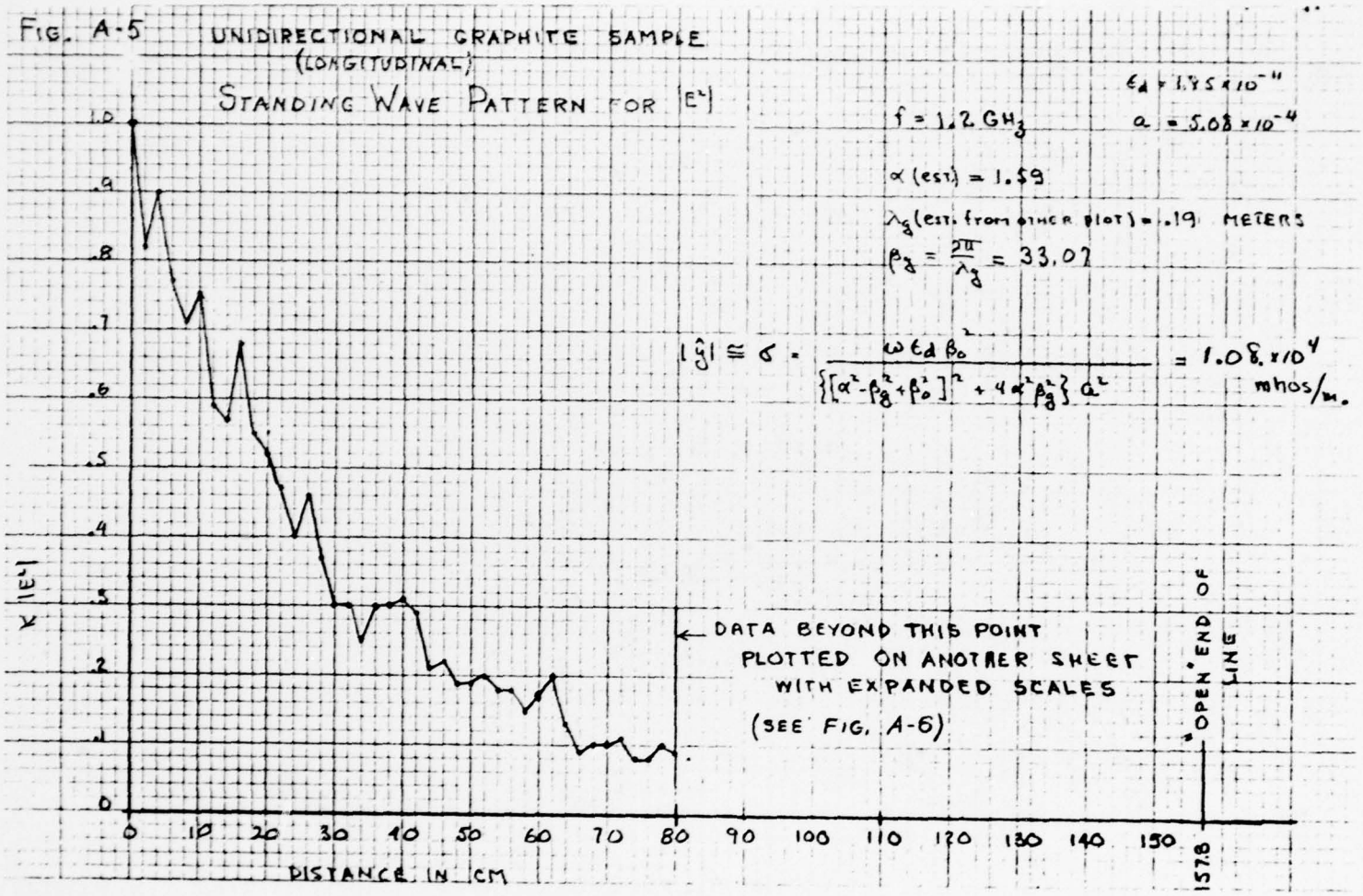
FIG. A-5 UNIDIRECTIONAL GRAPHITE SAMPLE
(LONGITUDINAL)
STANDING WAVE PATTERN FOR |E²|
$\epsilon_d = 1.75 \times 10^{-11}$
$a = 5.08 \times 10^{-4}$
$f = 1.2$ GHz
α (est.) = 1.59
λ_g (est. from other plot) = .19 METERS
$\beta_g = \frac{2\pi}{\lambda_g} = 33.07$
$|\hat{g}| \cong \sigma \cdot \frac{\omega \epsilon_d \beta_0^2}{\{[\alpha^2 - \beta_g^2 + \beta_0^2]^2 + 4\alpha^2\beta_g^2\} a^2} = 1.08 \times 10^4$ mhos/m.
|E²|
DATA BEYOND THIS POINT PLOTTED ON ANOTHER SHEET WITH EXPANDED SCALES
(SEE FIG. A-6)
OPEN END OF LINE
157.8
DISTANCE IN CM
0 10 20 30 40 50 60 70 80 90 100 110 120 130 140 150
0 .1 .2 .3 .4 .5 .6 .7 .8 .9 1.0

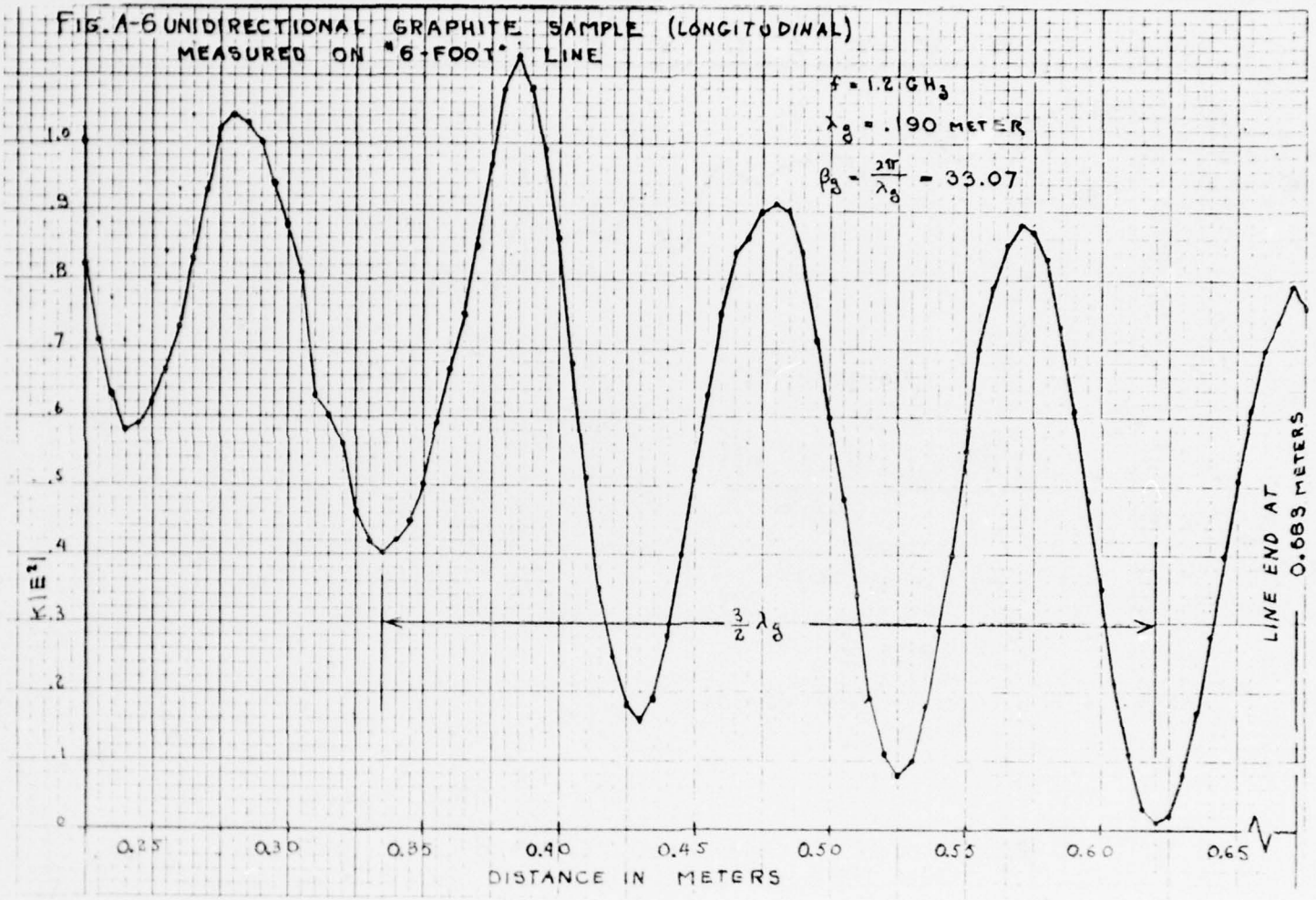
FIG. A-6 UNIDIRECTIONAL GRAPHITE SAMPLE (LONGITUDINAL)
MEASURED ON "6-FOOT" LINE
f = 1.2 GHz
λg = .190 METER
βg = 2π/λg = 33.07
|E²|
1.0
.9
.8
.7
.6
.5
.4
.3
.2
.1
0
3/2 λg
LINE END AT
0.683 METERS
0.25
0.30
0.35
0.40
0.45
0.50
0.55
0.60
0.65
DISTANCE IN METERS

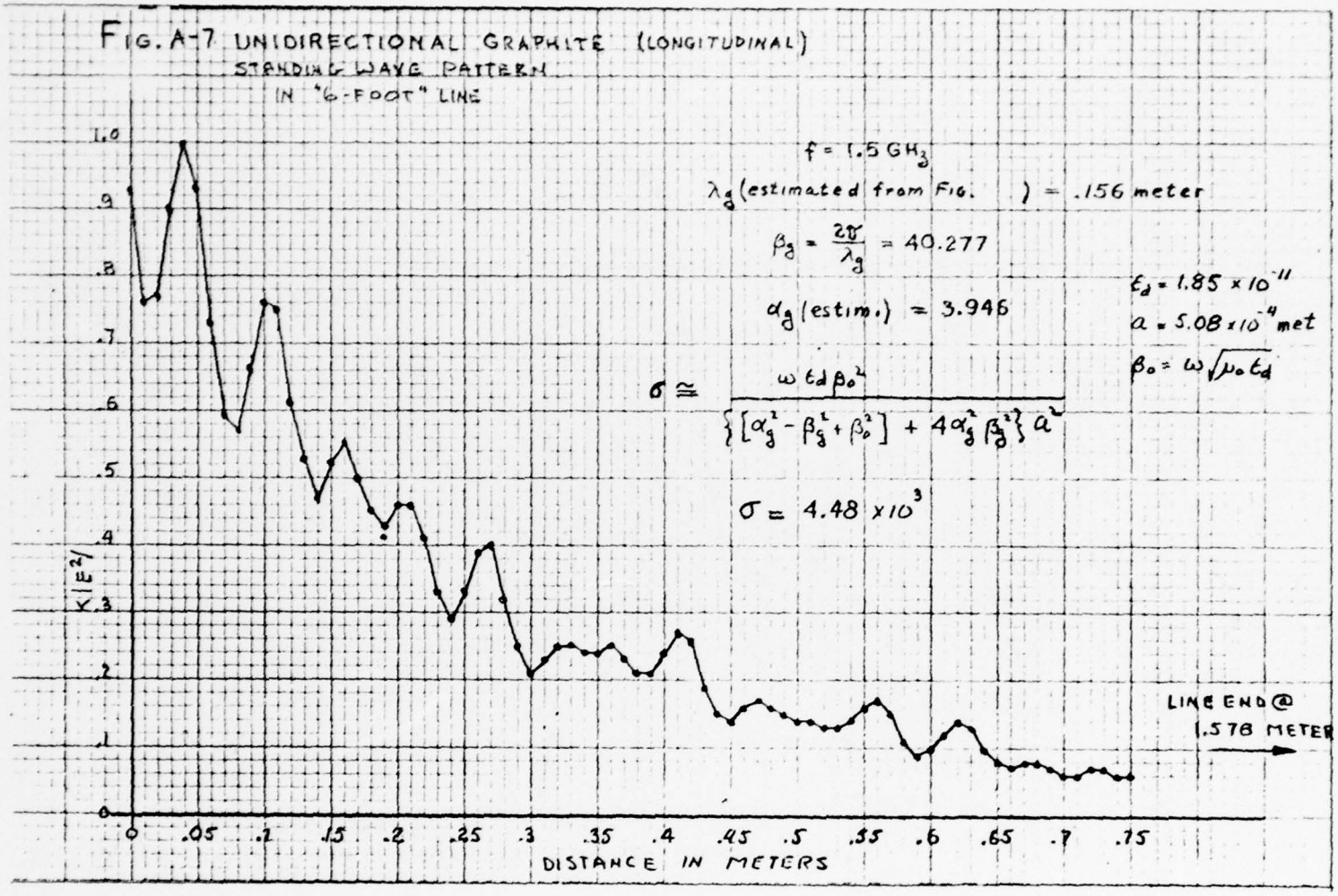
FIG. A-7 UNIDIRECTIONAL GRAPHITE (LONGITUDINAL)
STANDING WAVE PATTERN
IN "6-FOOT" LINE
f = 1.5 GHz
λg (estimated from Fig.) = .156 meter
βg = 2π/λg = 40.277
αg (estim.) = 3.946
εd = 1.85 × 10^-11
a = 5.08 × 10^-4 met
β0 = ω√(μ0 εd)
σ ≅ ω εd β0^2 / {[αg^2 - βg^2 + β0^2] + 4αg^2 βg^2} a^2
σ = 4.48 × 10^3
|E^2|/K
1.0
.9
.8
.7
.6
.5
.4
.3
.2
.1
0
0 .05 .1 .15 .2 .25 .3 .35 .4 .45 .5 .55 .6 .65 .7 .75
DISTANCE IN METERS
LINE END @ 1.578 METER

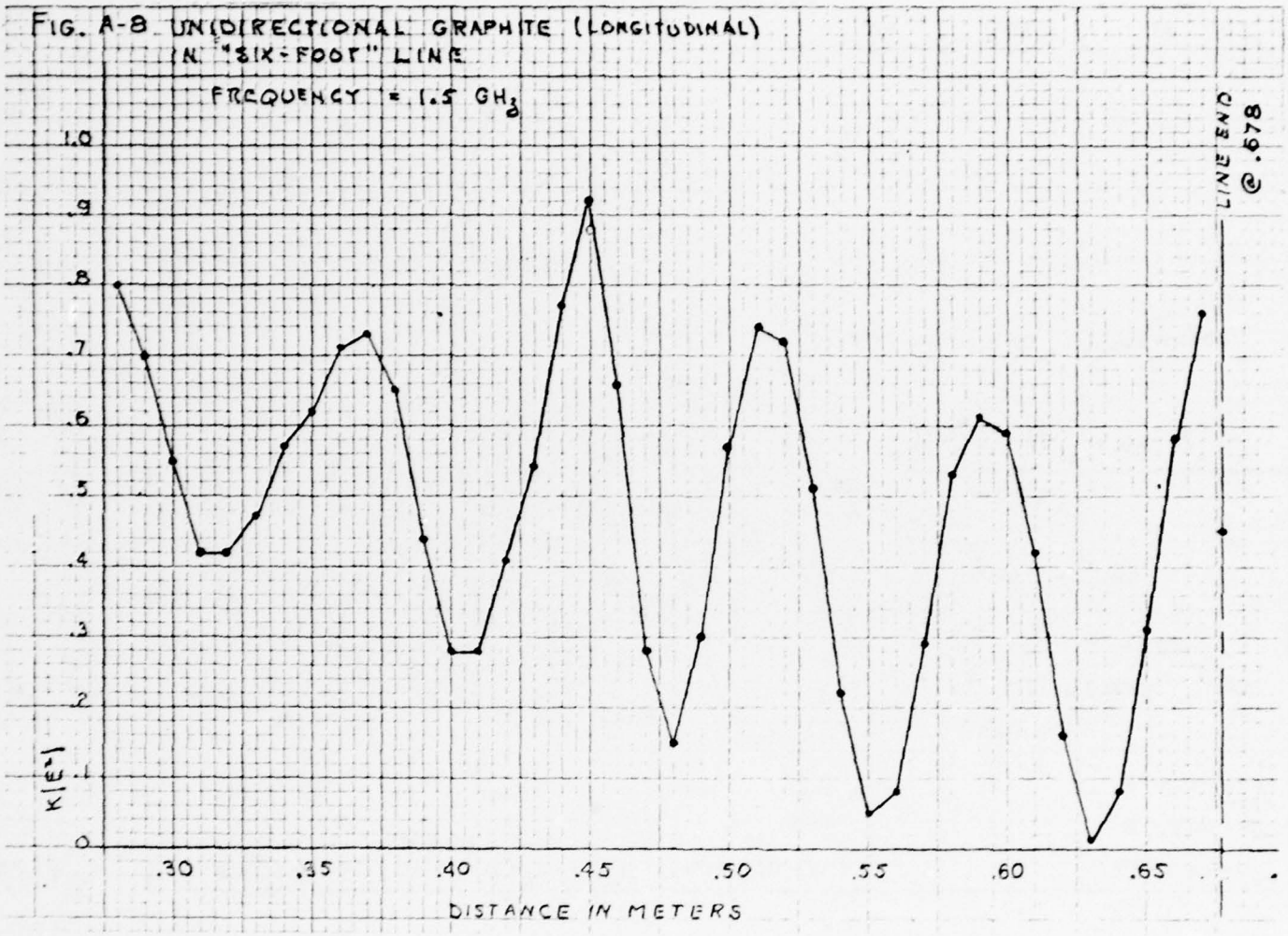
FIG. A-8 UNIDIRECTIONAL GRAPHITE (LONGITUDINAL)
IN "SIX-FOOT" LINE
FREQUENCY = 1.5 GHz
LINE END @ .678
K(E)
1.0
.9
.8
.7
.6
.5
.4
.3
.2
.1
0
.30
.35
.40
.45
.50
.55
.60
.65
DISTANCE IN METERS

FIG. A-9 UNIDIRECTIONAL GRAPHITE SAMPLE (LONGITUDINAL)
MEASURED ON "10-INCH" LINE

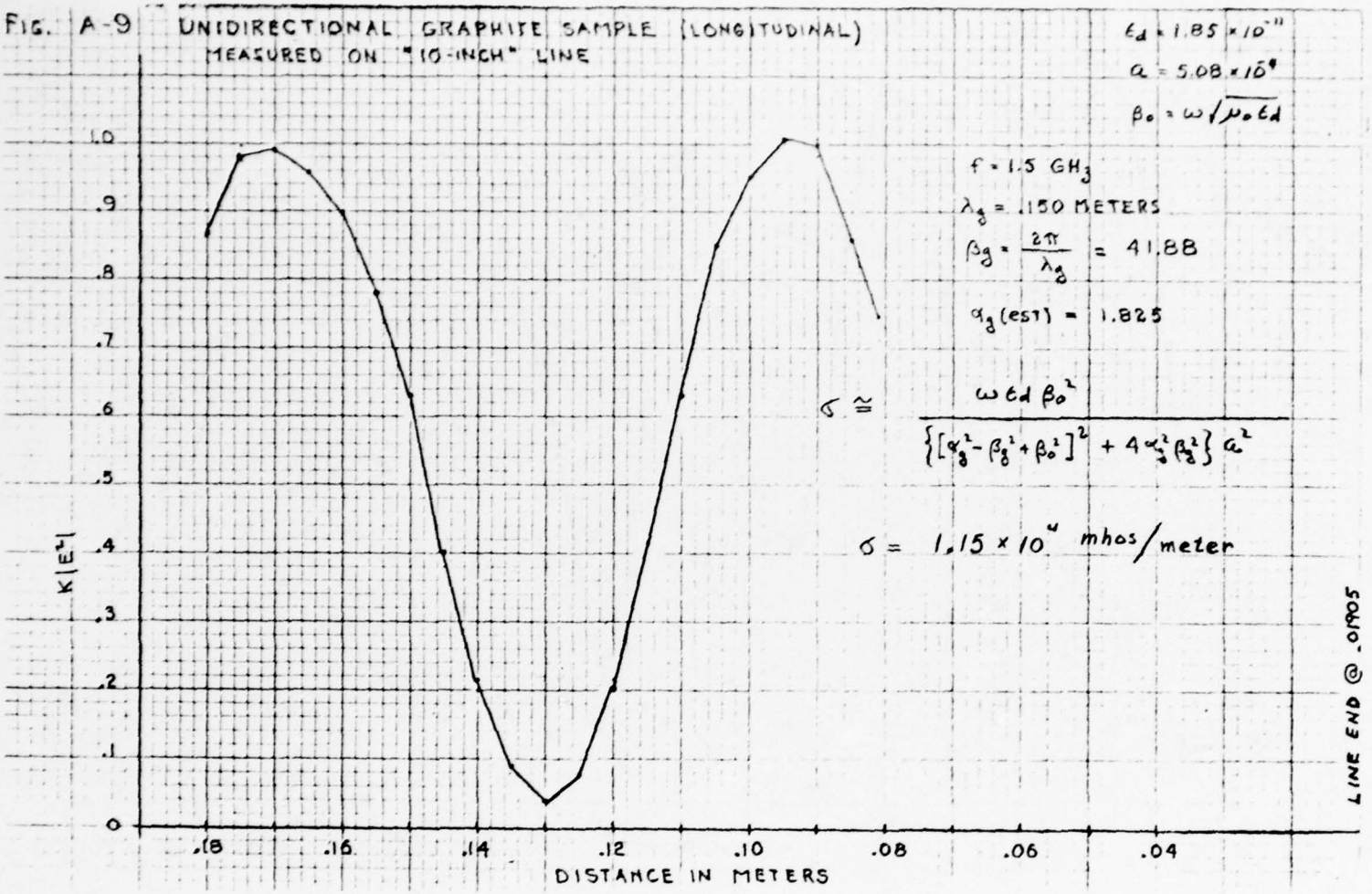

$\epsilon_d = 1.85 \times 10^{-11}$

$\alpha = 5.08 \times 10^{9}$

$\beta_o = \omega\sqrt{\mu_o \epsilon_d}$

$f = 1.5\ GH_3$

$\lambda_g = .150$ METERS

$\beta_g = \frac{2\pi}{\lambda_g} = 41.88$

$\alpha_g(est) = 1.825$

$$\sigma \approx \frac{\omega \epsilon_d \beta_o^2}{\left\{\left[\alpha_g^2 - \beta_g^2 + \beta_o^2\right]^2 + 4\alpha_g^2\beta_g^2\right\}\alpha^2}$$

$\sigma = 1.15 \times 10^{4}$ mhos/meter

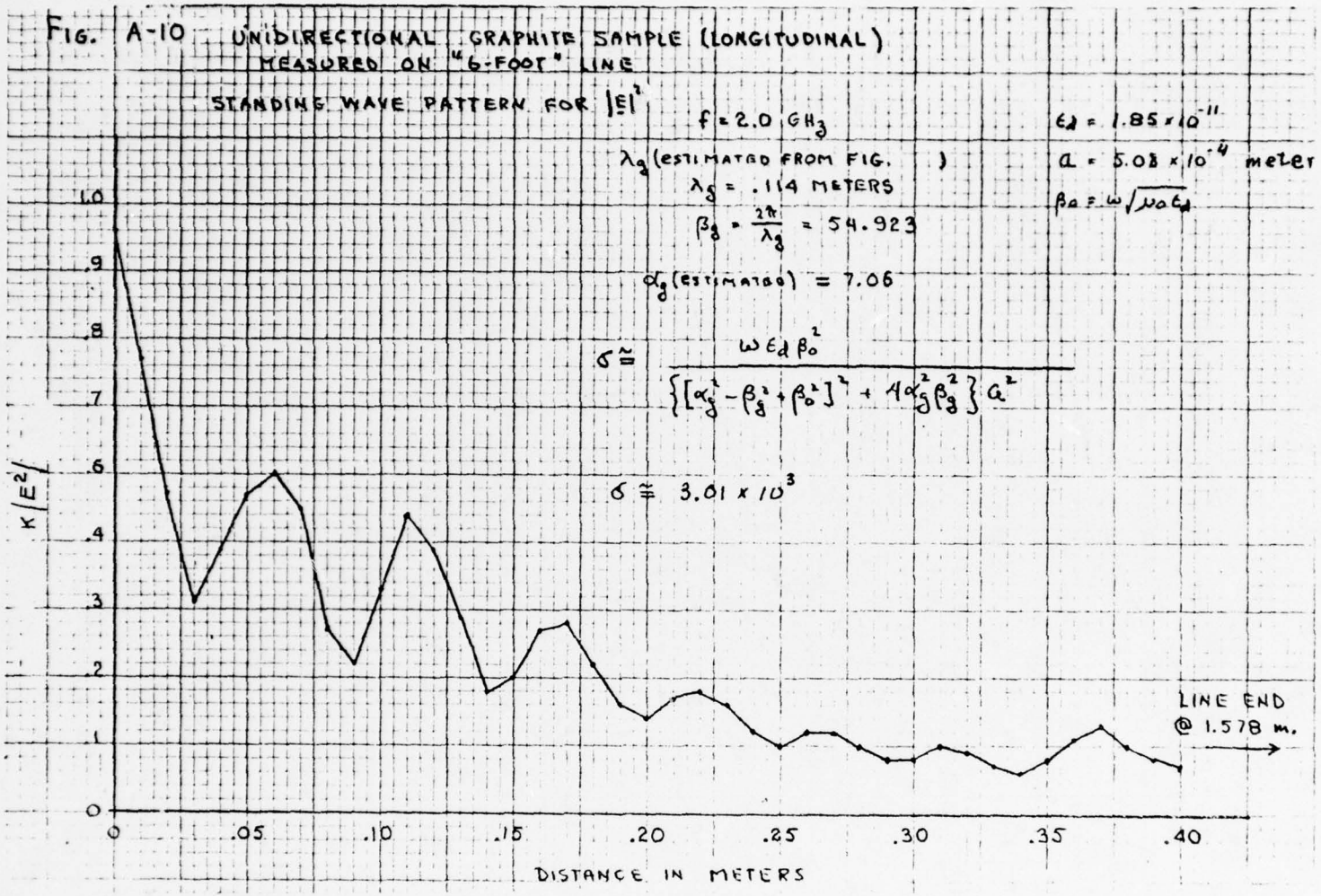
FIG. A-10 UNIDIRECTIONAL GRAPHITE SAMPLE (LONGITUDINAL)
MEASURED ON "6-FOOT" LINE
STANDING WAVE PATTERN FOR $|E|^2$
$f = 2.0$ GHz
λ_g (ESTIMATED FROM FIG.)
$\lambda_g = .114$ METERS
$\beta_g = \frac{2\pi}{\lambda_g} = 54.923$
α_g (ESTIMATED) $= 7.06$
$\sigma \cong \frac{\omega \epsilon_d \beta_o^2}{\{[\alpha_g^2 - \beta_g^2 + \beta_o^2]^2 + 4\alpha_g^2\beta_g^2\}a^2}$
$\sigma \cong 3.01 \times 10^3$
$\epsilon_d = 1.85 \times 10^{-11}$
$a = 5.08 \times 10^{-4}$ meter
$\beta_o = \omega\sqrt{\mu_o \epsilon_d}$
$K|E^2|$
0
.1
.2
.3
.4
.6
.7
.8
.9
1.0
0
.05
.10
.15
.20
.25
.30
.35
.40
DISTANCE IN METERS
LINE END
@ 1.578 m.

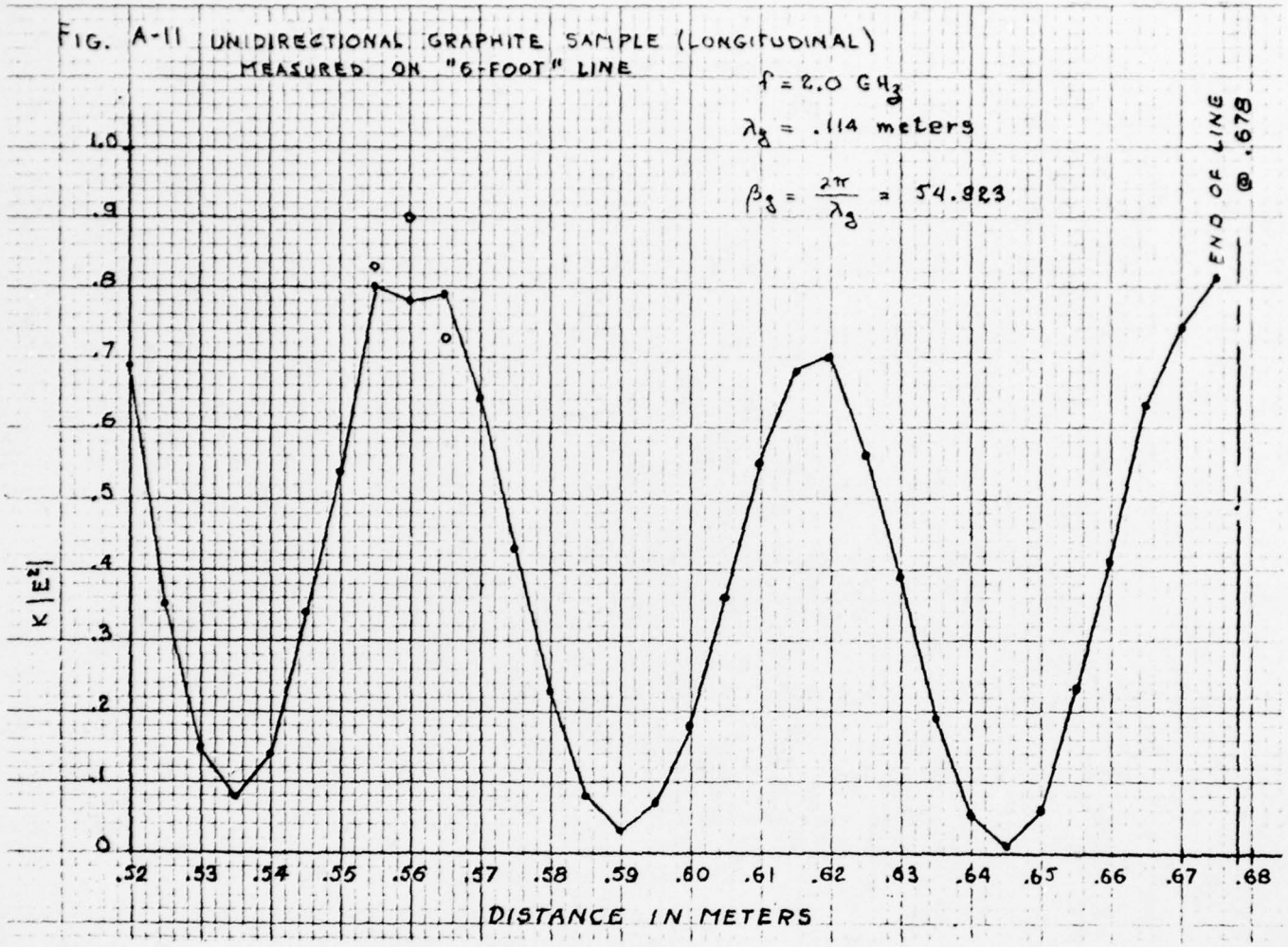
FIG. A-11 UNIDIRECTIONAL GRAPHITE SAMPLE (LONGITUDINAL)
MEASURED ON "6-FOOT" LINE
f = 2.0 GHz
λg = .114 meters
βg = 2π/λg = 54.823
END OF LINE @ .678
K |E²|
1.0
.9
.8
.7
.6
.5
.4
.3
.2
.1
0
.52 .53 .54 .55 .56 .57 .58 .59 .60 .61 .62 .63 .64 .65 .66 .67 .68
DISTANCE IN METERS

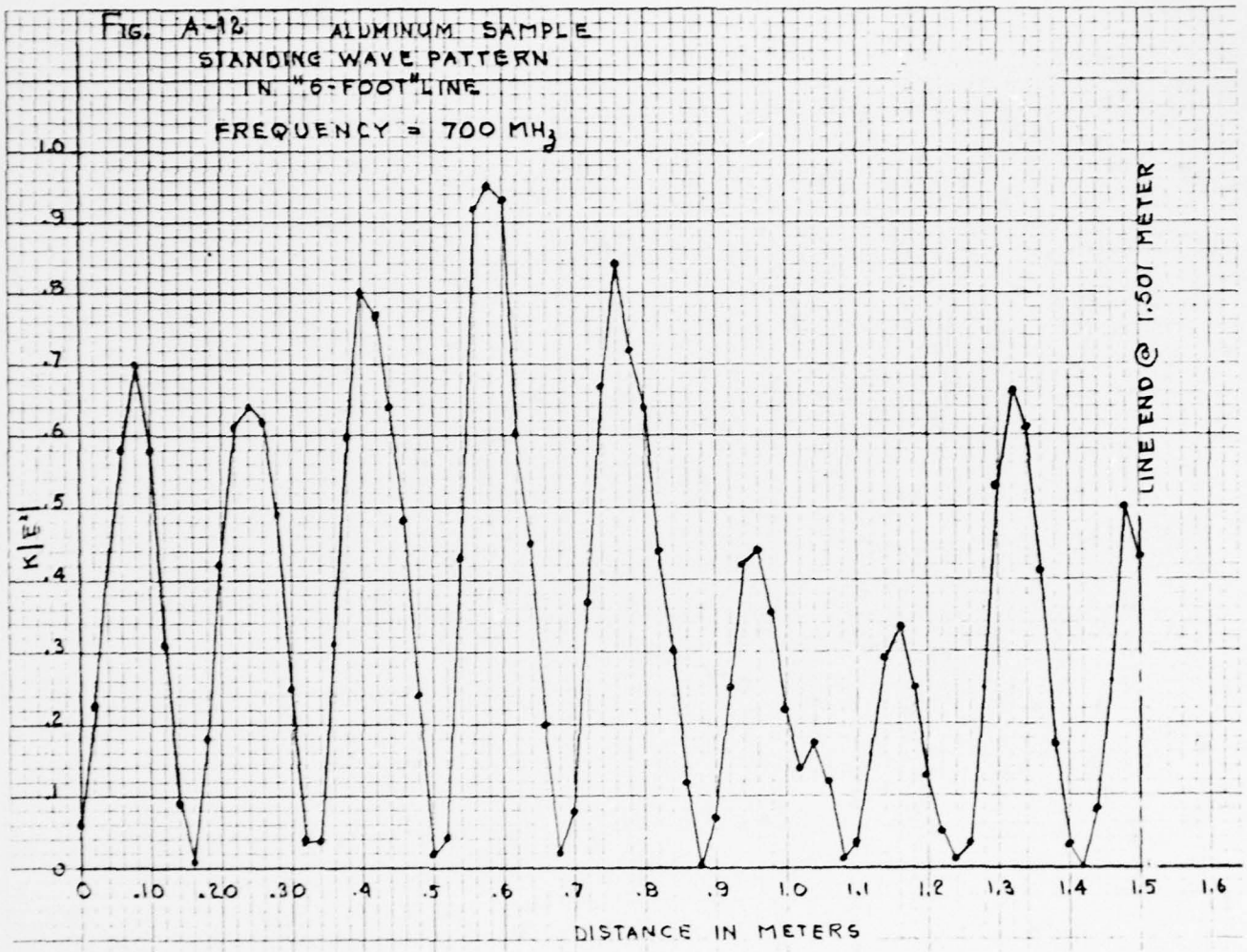
FIG. A-18 ALUMINUM SAMPLE
STANDING WAVE PATTERN
IN "6-FOOT" LINE
FREQUENCY = 700 MH3
K|E²|
LINE END @ 1.501 METER
0
.10
.20
.30
.4
.5
.6
.7
.8
.9
1.0
1.1
1.2
1.3
1.4
1.5
1.6
DISTANCE IN METERS

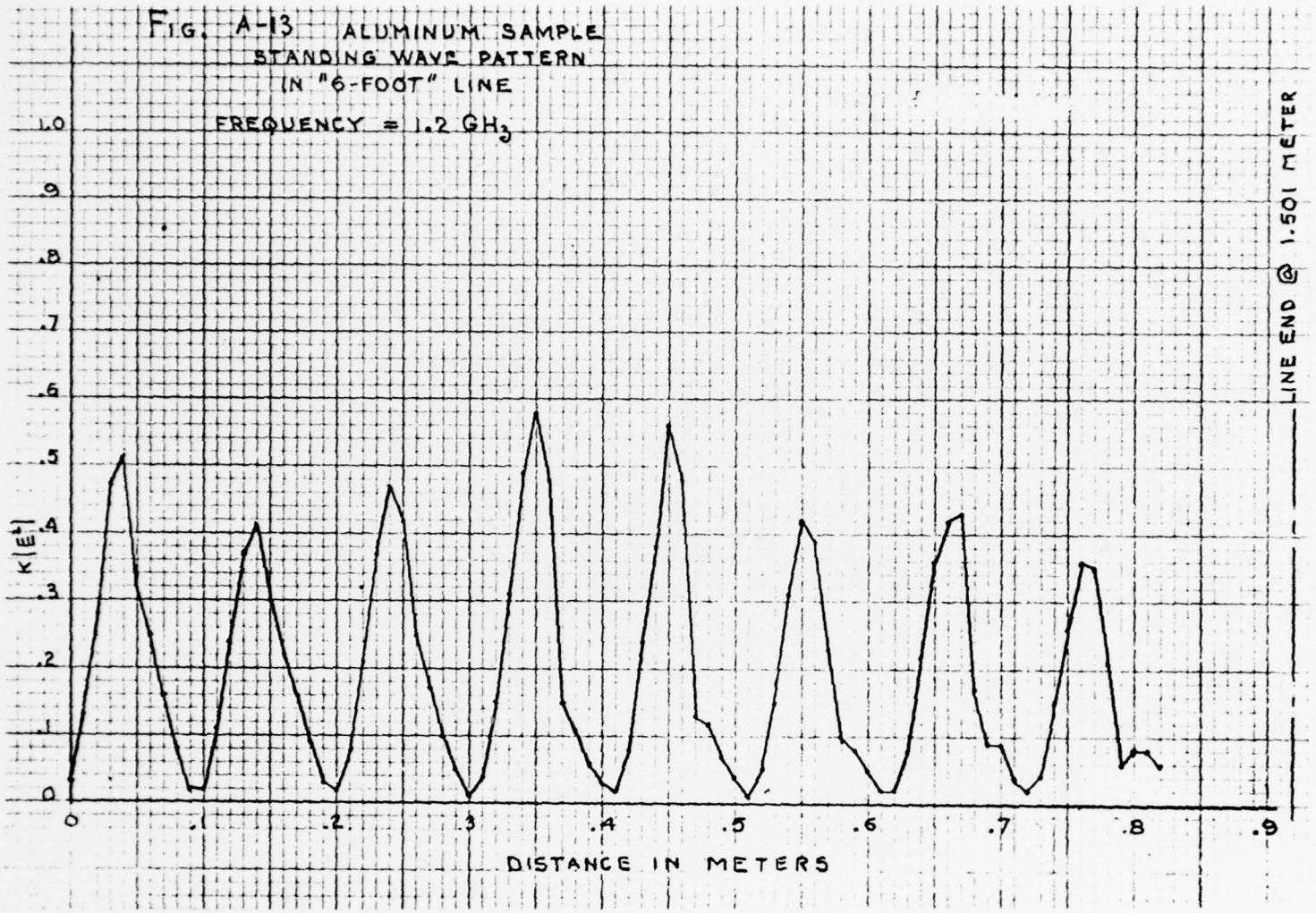
FIG. A-13 ALUMINUM SAMPLE
STANDING WAVE PATTERN
IN "6-FOOT" LINE
FREQUENCY = 1.2 GH3
K|E|
1.0
.9
.8
.7
.6
.5
.4
.3
.2
.1
0
0
.1
.2
.3
.4
.5
.6
.7
.8
.9
DISTANCE IN METERS
LINE END @ 1.501 METER

FIG. A-14 UNIDIRECTIONAL BORON (LONGITUDINAL) STANDING WAVE PATTERN ON "10-INCH" LINE

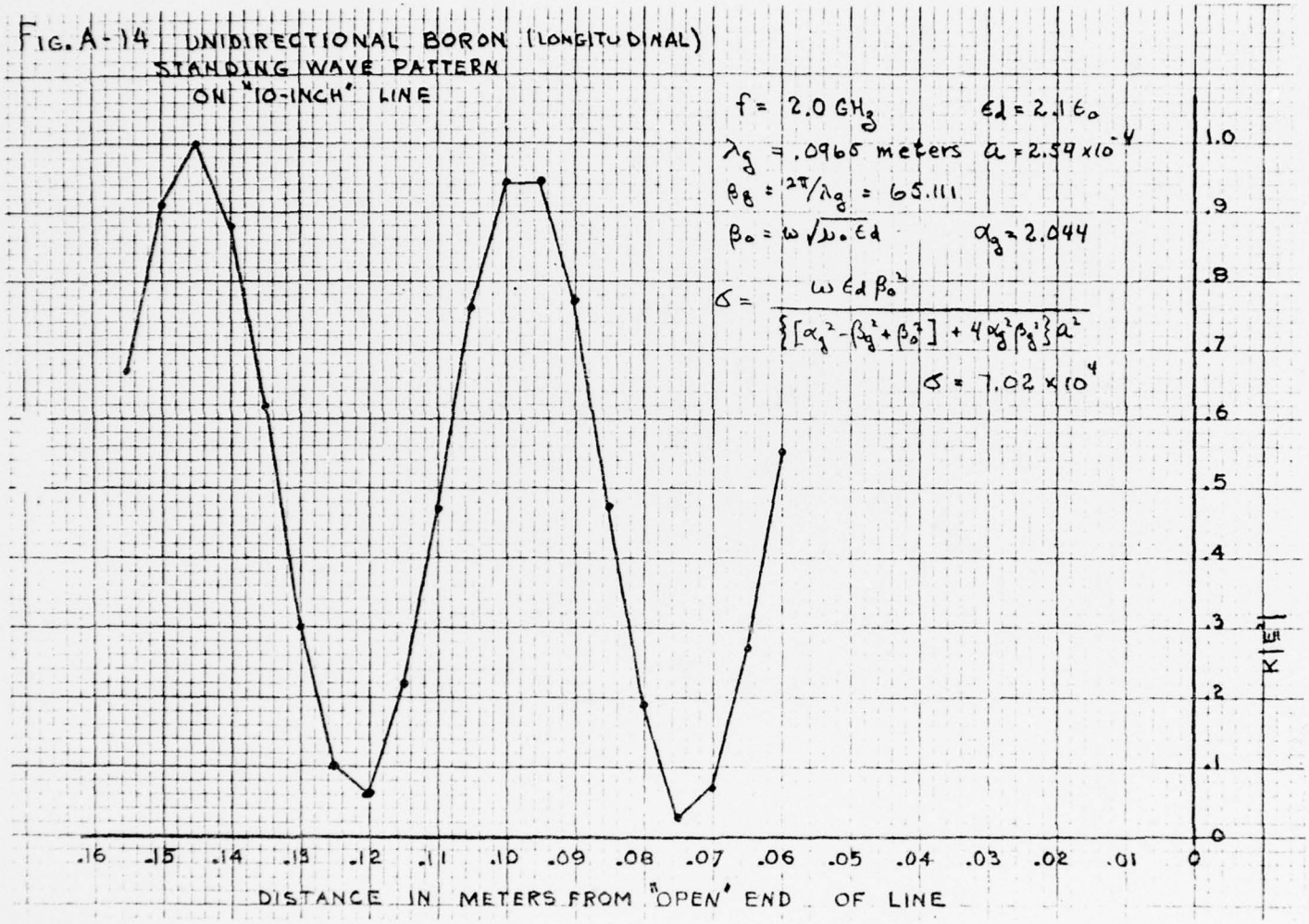

MISSION
of
Rome Air Development Center

RADC plans and executes research, development, test and selected acquisition programs in support of Command, Control Communications and Intelligence (C^3I) activities. Technical and engineering support within areas of technical competence is provided to ESD Program Offices (POs) and other ESD elements. The principal technical mission areas are communications, electromagnetic guidance and control, surveillance of ground and aerospace objects, intelligence data collection and handling, information system technology, ionospheric propagation, solid state sciences, microwave physics and electronic reliability, maintainability and compatibility.